

Quasi-linear theory of forced rotating sheared turbulence

Nicolas Leprovost and Eun-jin Kim

Department of Applied Mathematics, University of Sheffeld, Sheffeld S3 7RH, UK

May 27, 2019

Abstract

Rotation and shear flows are an ubiquitous features of many astrophysical and geophysical bodies, playing a crucial role in turbulent transport. To understand the complex dynamics in these systems, we provide a consistent theory of turbulence in the presence of shear and rotation. Starting from a quasi-linear equation for the fluctuating fields, we derive turbulence amplitude and turbulent transport coefficients (turbulent viscosity and diffusivity), taking into account the effect of shear and rotation on turbulence. We focus on the two cases where the rotation is perpendicular and parallel to the plane of the shear flow. We show that the shear reduces both turbulence amplitude and transport, more strongly in the direction parallel to the shear than in the perpendicular one, effectively inducing an anisotropic turbulence. The rotation further reduces turbulence amplitude and transport when it is perpendicular to the shear but does not have much effect when it is parallel to the shear. The interaction between the shear and the rotation is shown to give rise to a novel non-dissipative flux of angular momentum (effect), providing a mechanism for the permanence of shearing structure in astrophysical and geophysical systems. Eddy viscosity tends to become negative for fast rotation and strong shear. Anisotropic transport reduction is also found in turbulent mixing of passive scalars, largely due to shear flow.

1 Introduction

Rotating turbulent flows can be found in many areas such as engineering (turbomachinery, combustion engine), geophysics (oceans, Earth's atmosphere) or astrophysics (gaseous planets, galactic and accretion disks). Large-scale fluid motions tends to appear as a robust feature in these systems, often in the form of shear flows (such as circulations on the surface of planets, differential rotation in stars and galaxies or flows in a rotating machinery), which in turn plays a crucial role in determining turbulence properties and transport, such as energy transfer or mixing (Kim, 2005). The understanding of the complex interaction among rotation, large-scale shear flows and turbulence thus lies in the heart of the predictive theory of turbulent transport in many systems.

The case of the plane shear flow in a rotating frame has been studied by many authors focusing on its stability both in the laminar and the turbulent cases. In the case of a rotation vector $\tilde{\omega} = \tilde{\omega}_z \mathbf{e}_z$ perpendicular to the plane

of the shear flow, Bradshaw (1969) proposed an analogy between rotation and stratification [supported by calculation of Pedley (1969)] and showed that the system was unstable if the vorticity of the shear flow $A e_z$ is antiparallel to the rotation and sufficiently strong. Precisely, the ratio $\Omega = 2\tilde{\omega}A$ must lie in the interval $[0; 1]$ for instability. This destabilisation of laminar shear flow by rotation has a counterpart for turbulent flows where the rotation can stabilise turbulence (by decreasing its kinetic energy) or destabilise it. Theoretically Tritton (1992), by using a displacement argument, and Yanase et al. (1993), by using stability analysis confirmed by simulations (Métais et al., 1995), reach the following conclusion: the cyclonic shear ($\Omega < 0$) is always stabilising whereas the anticyclonic shear ($\Omega > 0$) is destabilising for weak rotation while stabilising for high rotation, in agreement with Bradshaw criterion. These conclusions are confirmed for a Poiseuille flow, both experimentally (Johnston et al., 1972) and numerically (Kristoffersen & Andersson, 1993), and for a plane Couette flow (Bech & Andersson, 1996, 1997). In comparison, the case where the rotation lies in the same plane as the flow has been much less studied. From the stability point of view, one could argue (e.g., Cambon et al., 1994; Leblanc & Cambon, 1997; Sipp & Jacquin, 2000) that as the projection of the vorticity on the rotation axis vanishes in this case (for a linear shear), the system may be stable regardless of the values of the rotation rate or shear.

Provided that a large-scale shear flow is stable, this flow and rotation have a crucial influence on the regulation of turbulent transport. The Taylor-Proudman theorem (Proudman, 1916; Taylor, 1921) states that for sufficiently strong rotation, the motion becomes independent of the coordinate along the rotation axis (in the linear inviscid regime). However, this linear theory does not permit to study the transition from three-dimensional to two-dimensional structures as rotation increases. In fact, Cambon et al. (1997) have shown that the turbulence energy concentrates in the plane normal to the rotation axis due to non-linear interactions. This could explain why a linear theory such as the rapid distortion theory (RDT) cannot capture the transition from three-dimensional to two-dimensional structures. Later, this result has been confirmed by the numerical simulations by Smith & Waleffe (1999), who showed that the large-scale energy lies mainly in two-dimensional modes due to non-linear interactions between inertial waves. However, they also showed that the inverse cascade of energy was mainly caused by non-local interactions between the large and small scale velocity fields. According to these results, a linear theory such as RDT should be able to capture the inverse cascade, if not the transition to two dimensions. This will be shown later in this paper.

In rotating turbulence, the inverse cascade can occur not only due to a (diffusive) negative viscosity, but also due to non-dissipative momentum transport. The latter is known as the anisotropic kinetic effect (AKA) (Frisch et al., 1987) or as the effect in the astrophysical community. The appearance of non-dissipative term in the transport of angular momentum prevents a solid body rotation from being a solution of the Reynolds equation (Lebedinsky, 1941; Kippenhahn, 1963), and thus act as a source for the generation of large-scale shear flows. For instance, this effect has been advocated as a robust mechanism to explain the differential rotation in the solar convective zone. Starting from Navier-Stokes equation, it is possible to show that these vortices arise when there is a cause of anisotropy in the system, either due to an anisotropic background turbulence (see Rudiger, 1989, and references therein) or else due to

inhomogeneities such as an underlying stratification (Kichatinov, 1987).

Another important problem, which have received much less attention, is the effect of rotation and shear on the mixing and transport of scalars (such as pollutants, heat or reacting species). For instance, observations show that the concentration of light elements at the surface of the Sun is smaller than what is expected by comparison with Earth's or meteorites abundance. As these light elements can only be destroyed below the strong shearing region (the tachocline), it is crucial to understand the transport properties of scalars in a rotating sheared layer. Note that studies of passive scalar transport in non-rotating sheared turbulence (Tavoularis & Corrsin, 1981; Rogers et al., 1989) have shown a strong misalignment between the scalar flux and the mean gradient. Thus, gradient-diffusion models are not very appropriate to study the evolution of a large-scale scalar gradient. In comparison, in rotating turbulence, Brethouwer (2005) found that numerical simulation results agree fairly well with linear theory and showed that the scalar flux vector aligned itself in the direction of strongest velocity fluctuation.

The main purpose of this paper is to investigate the effect of rotation and shear flow on the turbulence properties and transport. In our previous works, we have studied the turbulent transport by taking into account the crucial effect of shearing, the so-called shear stabilisation, due to a strong radial differential rotation (Kim, 2005; Leprovost & Kim, 2006) and also by incorporating the interaction of this sheared turbulence with different types of waves that can be excited due to magnetic fields (Kim & Dubrulle, 2001; Kim, 2006; Leprovost & Kim, 2007) or stratification (Kim & Leprovost, 2006). Here, we study a (local) Cartesian model concentrating on the two cases where the shear direction and the rotation are perpendicular or parallel to each other. We consider a turbulence driven by an external forcing and perform a quasi-linear analysis to derive the dependence of turbulence amplitude and transport on rotation and shear. Compared to two-dimensional turbulence studied in Leprovost & Kim (2007), the (average) rotation supports the propagation of inertial waves in three dimensions, which interact with a shear flow, playing an important role in the overall turbulent transport. In particular, we show that the momentum transport is not only due to eddy-viscosity but also to non-dissipative effect. Non-trivial effect can result from an anisotropy induced by shear flow on the turbulence even when the driving force is isotropic, in contrast to the case without shear flow where this effect exists only for anisotropic turbulence (Kichatinov, 1987). Furthermore, the eddy-viscosity can change its sign depending on the relative strength of rotation, shear and dissipation. We also examine the effect of rotation on the stability of shear flows.

The remainder of the paper is organised as follows: in §2, we provide the quasi-linear equations for the fluctuating velocity and density of particles in a rotating frame with an arbitrary external forcing. We then proceed to the calculations of the turbulent intensity and turbulent transport in the case where shear and rotation are perpendicular (§3) or parallel (§4) to each other. We then discuss our findings in the strong shear limit (§5) and provide concluding remarks in §6.

2 Model

Our model is an incompressible fluid in a rotating frame with average rotation rate Ω . The main governing equations are:

$$\begin{aligned} \partial_t \mathbf{u} + \mathbf{u} \cdot \nabla \mathbf{u} &= -\nabla p + \nu \nabla^2 \mathbf{u} + \mathbf{F} - 2\boldsymbol{\Omega} \times \mathbf{u}; \\ \nabla \cdot \mathbf{u} &= 0; \end{aligned} \quad (1)$$

To simplify notation, we let $\Omega = 2\tilde{\Omega}$. In Cartesian coordinates, the Coriolis force can be written as:

$$\mathbf{u} = u_x \sin \theta \hat{i} + (u_x \sin \theta - u_y \cos \theta) \hat{j} + u_y \cos \theta \hat{k}; \quad (2)$$

where \hat{i} , \hat{j} and \hat{k} are the unit vectors associated to the Cartesian coordinates. θ is chosen to lie in the plane $y = 0$ and to make an angle θ with the z direction. Following Kim (2005), we study the effect of a large-scale shear $U_0 = U_0(x)\hat{j}$ on the transport properties of turbulence by writing the velocity as a sum of a shear (chosen in the x -direction) and fluctuations: $\mathbf{u} = U_0 + \mathbf{v} = U_0(x)\hat{j} + \mathbf{v} = xA\hat{j} + \mathbf{v}$. Without loss of generality, we assume $A > 0$.

To calculate the turbulence amplitude (or kinetic energy growth) and the turbulent viscosity, we need to solve the equation for the fluctuating velocity field. We resort to the quasi-linear approximation (Moffatt, 1978) where the product of fluctuations is neglected to obtain the following equations for the evolution of the fluctuating velocity field:

$$\begin{aligned} \partial_t \mathbf{v} + U_0 \cdot \nabla \mathbf{v} + \mathbf{v} \cdot \nabla U_0 &= -\nabla p + \nu \nabla^2 \mathbf{v} + \mathbf{f} - 2\boldsymbol{\Omega} \times \mathbf{v}; \\ \nabla \cdot \mathbf{v} &= 0; \end{aligned} \quad (3)$$

where p and \mathbf{f} are respectively the small-scale components of the pressure and forcing. This approximation, also known as rapid distortion theory (Townsend, 1976) is strictly valid only for two-scale turbulence, with a spatial gap between a large-scale for the shear and a small scale for the fluctuating velocity, and for weak turbulence. However, it is likely to be valid in our case as the large-scale shear induces a weak turbulence, leading to weak interaction between small scales which is negligible compared to the (non-local) interaction between the shear and the small scales. This has in fact been confirmed by direct numerical simulations showing the validity of the predictions of quasi-linear theory with a constant-rate shear both in the non-rotating (Lee et al., 1990) and rotating (Sahi & Cambon, 1997) case.

To solve equation (3), we introduce a Fourier transform with a wave number in the x direction evolving in time in order to compute non-perturbatively the effect of the advection by the mean shear flow (Goldreich & Lynden-Bell, 1964; Townsend, 1976; Kim, 2005):

$$\mathbf{v}(\mathbf{x}; t) = \frac{1}{(2\pi)^2} \int d^3k e^{i[k_x(t)x + k_y y + k_z z]} \hat{\mathbf{v}}(\mathbf{k}; t); \quad (4)$$

where $k_x(t) = k_x(0) + k_y A t$. From equations (3) and (4), we obtain the following set of equations for the fluctuating velocity:

$$\begin{aligned} A \partial_t \hat{v}_x &= ik_y \hat{p} + \hat{f}_x + \hat{v}_y \sin \theta; \\ A \partial_t \hat{v}_y - A \hat{v}_x &= ik_y \hat{p} + \hat{f}_y + (\hat{v}_z \cos \theta - \hat{v}_x \sin \theta); \\ A \partial_t \hat{v}_z &= ik_z \hat{p} + \hat{f}_z - \hat{v}_y \cos \theta; \\ 0 &= \hat{v}_x + \hat{v}_y + \hat{v}_z; \end{aligned} \quad (5)$$

Here, the new variables $\hat{v} = v \exp[(k_y^2 t + k_x^3 = 3k_y A)]$ and similarly for \hat{f} and \hat{p} have been used to absorb the dispersive term, and the time variable has been changed to $t = k_x(t) = k_y$. In the remainder of the paper, we solve equation (5) for the fluctuating velocity (with a vanishing velocity as initial condition) in the case where the shear and the average rotation are perpendicular (x3) or parallel (x4). We then use these results and the correlation of the forcing (defined in x2.3) to compute the turbulence intensity and transport (defined in x2.2). We divide our study into four cases depending on the relative magnitude of the three characteristic frequencies in the problem: the diffusion rate (k^2), the rotation rate and the shearing rate A . We first consider the case of large ($A > k^2$) and weak rotation ($A < k^2$). For each of these cases, we consider the large ($A > k^2$) and weak ($A < k^2$) shear limits.

2.1 Transport of angular momentum

As the large-scale velocity is in the y direction, we are mostly interested in the transport in that direction. The large-scale equation for the y component of velocity U_0 is given by equation (1) with a supplementary term $r = R$ where R is the Reynolds stress given by:

$$R = \langle v v_y \rangle_i \quad (6)$$

To understand the effect of R on the transport of angular momentum, one can formally Taylor expand it with respect to the gradient of the large-scale flow:

$$R_i = \langle v v_y \rangle_i U_0 + \langle v v_y \rangle_{ix} U_{0,x} + \langle v v_y \rangle_{i0} + \langle v v_y \rangle_{ix} A + \dots \quad (7)$$

where we introduced two transport coefficients $\langle v v_y \rangle_i$ and $\langle v v_y \rangle_{ix}$. The effect of the turbulent viscosity $\langle v v_y \rangle_{ix}$ is simply to change the viscosity from the molecular value to the effective value $\nu + \langle v v_y \rangle_{ix}$. Note that rotation may give a negative turbulent viscosity, in which case the turbulent diffusion generates velocity gradients rather than smooths them out. In comparison, the first term in equation (7) is proportional to the velocity rather than its gradient. This means that it does not vanish for a constant velocity field and thus permits the creation of gradient in the large-scale velocity field. This term is the equivalent to the effect in dynamo theory (Parker, 1955; Steenbeck & Krause, 1966) and has been known as the α -effect (Lebedinsky, 1941; Rudiger, 1980) or anisotropic kinetic α (AKA)-effect (Frisch et al., 1987). Symmetry property of equation (7) shows that $\langle v v_y \rangle_{ix}$ is a polar vector and thus must change sign when going from right-handed to left-handed coordinates. This explains why this tensor cannot be present in purely isotropic turbulence but can exist for an helical turbulence [like the α -effect]. In the presence of rotation and anisotropy of the background medium, the turbulence is likely to be helical, possibly leading to α -effect.

2.2 Particle (or heat) transport

To study the influence of rotation and shear on the particle and heat transport, we have to supplement equation (1) with an advection-diffusion equation for these quantities. We here focus on the transport of particles since a similar result also holds for the heat transport. The density of particles $N(x;t)$ is

governed by the following equation:

$$\partial_t N + U \cdot \nabla N = D \nabla^2 N ; \quad (8)$$

where D is the molecular diffusivity of particle. Note that, in the case of heat equation, D should be replaced by the molecular heat conductivity. Writing the density as the sum of a large-scale component N_0 and small-scale fluctuations n ($N = N_0 + n$), we can express the evolution of the transport of chemicals on large-scale by:

$$\partial_t N_0 + U_0 \cdot \nabla N_0 = (D_{ij} + D_T^{ij}) \partial_i \partial_j N_0 ; \quad (9)$$

where the turbulent diffusivity is defined as $\langle n v_i n_i \rangle = D_T^{ij} \partial_j N_0$. Our study of turbulent transport of chemicals consists of deriving D_T^{ij} which, owing to rotation and shear, is likely to be highly anisotropic.

For simplicity, we limit our analysis to the case of a unit Prandtl number $D = \nu = \kappa$. In that case, we can apply the transformation introduced in equation (4) to the density fluctuation n and obtain the following equation:

$$\partial_t \hat{n} = \frac{(\partial_j N_0)}{A} \hat{v}_j ; \quad (10)$$

Equation (10) simply shows that the fluctuating density of particles can be obtained by integrating the fluctuating velocity in time.

2.3 External forcing

As mentioned in introduction, we consider a turbulence driven by an external forcing f . To calculate the turbulence amplitude and transport defined in x2.1 and x2.2, we need the two point correlation of this forcing (as all the quantities of interest involve quadratic functions of velocity and/or density). For simplicity, we prescribe this forcing to be short correlated in time (modelled by a δ -function) with power spectrum ϕ_{ij} in the Fourier space. Specifically, we assume:

$$\langle f_i(k_1; t_1) f_j(k_2; t_2) \rangle = \phi_{ij}(k) \delta(k_1 + k_2) \delta(t_1 - t_2) \phi_{ij}(k_2) ; \quad (11)$$

for i and $j = 1, 2$ or 3 . The angular brackets stand for an average over realisations of the forcing, and τ_f is the (short) correlation time of the forcing.

From most results that will be derived later, we assume an incompressible and isotropic forcing where the spectrum of the forcing is given by:

$$\phi_{ij}(k) = F(k) \delta_{ij} \delta(k_3) \delta(k^2) ; \quad (12)$$

It is easy to check that in the absence of rotation and shear, this forcing leads to an isotropic turbulence with intensity:

$$\langle n_0^2 \rangle = \frac{2\tau_f}{(2\pi)^2} \int_0^{\infty} F(k) dk ; \quad (13)$$

where the subscript 0 stands for a turbulence without shear and rotation.

In addition to an isotropic forcing, we will also consider an anisotropic forcing in x3.1.2 to examine the combined effect of rotation and anisotropy, which can lead to non-diffusive fluxes of angular momentum. Specifically, we consider an extremely anisotropic forcing with motion restricted to a plane perpendicular to

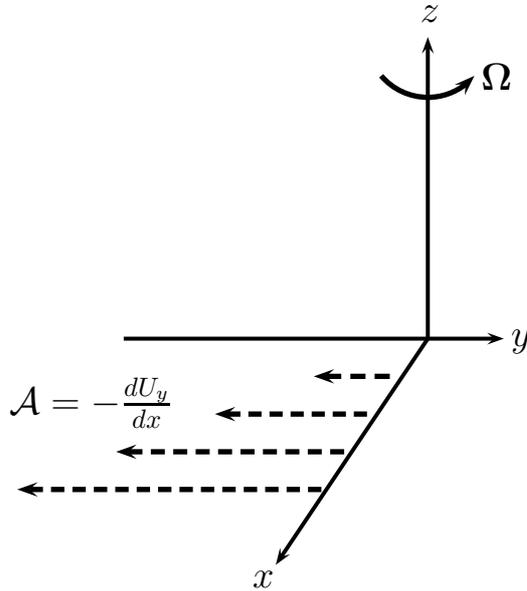


Figure 1: Sketch of the con guration in the perpendicular case

a given direction g . The motion in this perpendicular plane is however assumed to be isotropic. Such a forcing can be modelled by the following power spectrum (Rudiger, 1989):

$$h_{ij}(k) = G(k) \left[\delta_{ij} \frac{k_i k_j}{k^2} - \frac{(g_i k_j - g_j k_i)}{k^2} \right] \quad (14)$$

In that case, the turbulence without rotation or shear would have the following properties:

$$\begin{aligned} h(v_0 \cdot g)_i &= 0; \\ h(v_0 \cdot g)_i^2 &= \frac{2}{3} \frac{g^2}{(2\pi)^2} \int_0^{\infty} G(k) dk; \end{aligned} \quad (15)$$

3 The perpendicular case ($\beta = 2$)

In this section, we study the combined effect on turbulence of global rotation and shear which are perpendicular to each other (see figure 1).

For $\beta = 2$, the system (5) can be simplified to:

$$\begin{aligned} \partial^2 (\hat{v}_x + \hat{v}_y) + \Omega^2 (\hat{v}_x - \hat{v}_y) &= \partial \frac{h_1(\omega)}{A} \hat{v}_x + \frac{h_2(\omega)}{A}; \\ \partial \hat{v}_z &= -\partial \hat{v}_x + \frac{1}{\omega} \hat{v}_x + \frac{h_2(\omega)}{A}; \\ \hat{v}_y &= (\hat{v}_x + \hat{v}_z); \end{aligned} \quad (16)$$

Here:

$$\begin{aligned} &= A; \quad = k_z = k_y; \quad = 1 + \quad = k_H^2 = k_Y^2 \quad (k_H^2 = k_Y^2 + k_z^2) \quad (17) \\ h_1(\eta) &= \hat{f}_x \quad \hat{f}_y \quad \hat{f}_z; \quad h_2(\eta) = \hat{f}_z \quad \hat{f}_y : \end{aligned}$$

To solve the first of equation (16) which is a non-homogeneous second order differential equation, we need two boundary conditions. We impose $v(\eta) = 0$ which implies $\hat{v}_x(\eta) = 0$ and $\partial \hat{v}_x / \partial \eta = h_1(\eta) = (1 + \frac{\eta^2}{b^2})A$. The second boundary condition was obtained in the intermediate steps of deriving equation (16).

The exact solution of the homogeneous part of equation for the velocity \hat{v}_x can be found in terms of generalised hyper-geometric function $F([a_1; a_2; \dots]; [b_1; b_2; \dots]; x)$ (Gradshteyn & Ryzhik, 1965). Two independent solutions are:

$$\begin{aligned} X_1(\eta) &= F\left(\frac{h_3}{4} + \frac{\sqrt{1-4b}}{4}; \frac{3}{4}; \frac{\sqrt{1-4b}^i}{4}; \frac{h_1}{2}; \frac{\eta^2}{b^2}\right); \\ X_2(\eta) &= F\left(\frac{h_5}{4} + \frac{\sqrt{1-4b}}{4}; \frac{5}{4}; \frac{\sqrt{1-4b}^i}{4}; \frac{h_3}{2}; \frac{\eta^2}{b^2}\right); \end{aligned} \quad (18)$$

Here, $b = \frac{\eta^2}{b^2} (1)$ is (up to the multiplicative constant η^2) the quantity introduced by Bradshaw (1969) (see discussion in the introduction). Figure 2 shows the evolution of these two functions as a function of η .

Solutions for the other components of the velocity are obtained by using the last two equations of (16):

$$\begin{aligned} \hat{v}_y &= \frac{1}{b} X_n(\eta) + \eta^2 (1) Y_n(\eta); \\ \hat{v}_z &= - X_n(\eta) - (1) Y_n(\eta); \end{aligned} \quad (19)$$

for $n = 1$ or 2 . Here, Y_1 and Y_2 are defined as:

$$\begin{aligned} Y_1(\eta) &= F\left(\frac{h_3}{4} + \frac{\sqrt{1-4b}}{4}; \frac{3}{4}; \frac{\sqrt{1-4b}^i}{4}; \frac{h_3}{2}; \frac{\eta^2}{b^2}\right); \\ Y_2(\eta) &= \frac{1}{b} F\left[\frac{1}{4}; \frac{\sqrt{1-4b}}{4}; \frac{1}{4} + \frac{\sqrt{1-4b}}{4}; \frac{1}{2}\right]; \frac{\eta^2}{b^2}; \end{aligned} \quad (20)$$

The plots of $Y_1(\eta)$ and $Y_2(\eta)$ are shown in figure 3.

Figure 3 shows that the eigenfunctions diverge for $\eta \rightarrow 1$ when $b < 0$. This is because shear flows in presence of rotation (perpendicular to the shear flow) is stable only for $b > 0$. This result agrees with Bradshaw (1969) and Salhi & Cambon (1997). We can also notice that the solution with $b > 0$ always decays faster than that with $b < 0$.

Unfortunately, computations of correlation functions with this exact solution turns out to be too complex to be analytically tractable. To gain a physical insight into the problem, we consider the two regimes of the strong and weak (compared to shear) rotation limits, where approximate solutions can be derived and then be used for deriving analytic results for the correlation functions.

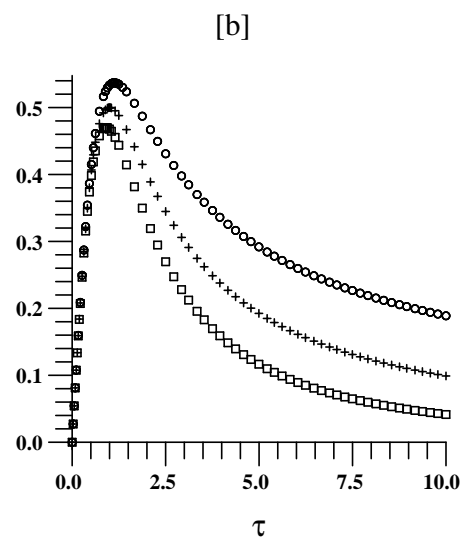
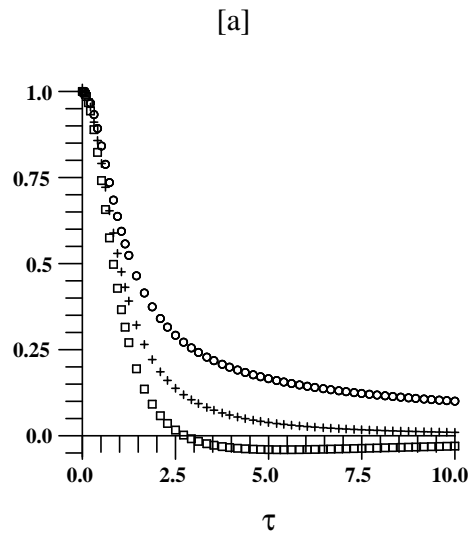


Figure 2: Evolution of the solution X_1 (panel [a]) and X_2 (panel [b]) as a function of τ for $b = 0.5$ (circles), $b = 0$ (crosses) and $b = 0.5$ (squares).

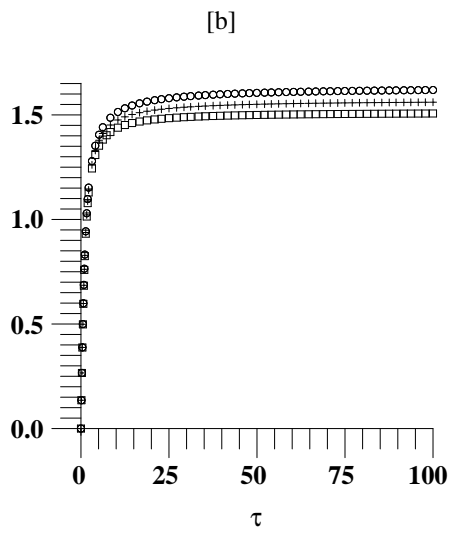
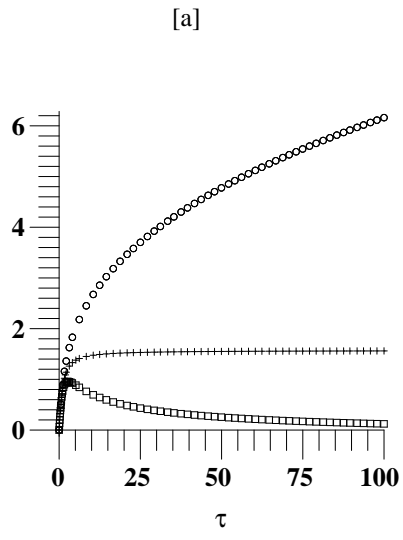


Figure 3: Evolution of the solution Y_1 (panel [a]) and Y_2 (panel [b]) as a function of τ for $b = 0.5$ (circles), $b = 0$ (crosses) and $b = 0.5$ (squares).

3.1 Strong rotation limit: $\Omega \rightarrow \infty$

When the rotation rate is much larger than shearing rate ($\Omega = \omega \tau_A \gg 1$), we can use a WKB approximation (Bender & Orszag, 1975). After a long but straightforward algebra, the solution of equation (16) can be found as:

$$\begin{aligned} \hat{v}_x(\mathbf{k}; t) &= \frac{1}{A(\omega^2 + \alpha^2)^{3/4}} \int_0^t dt \frac{\hat{h}_1(t)}{(\omega + \alpha^2)^{1/4}} \cos[\nu(\mathbf{k}; t)] + \hat{h}_2(t) (\omega + \alpha^2)^{1/4} \sin[\nu(\mathbf{k}; t)]; \\ \hat{v}_y(\mathbf{k}; t) &= \frac{1}{A(\omega^2 + \alpha^2)^{3/4}} \int_0^t dt \frac{\hat{h}_1(t)}{(\omega + \alpha^2)^{1/4}} \cos[\nu(\mathbf{k}; t)] + \frac{\omega}{\omega^2 + \alpha^2} \sin[\nu(\mathbf{k}; t)] \\ &\quad + \hat{h}_2(t) (\omega + \alpha^2)^{1/4} \sin[\nu(\mathbf{k}; t)] + \frac{\omega}{\omega^2 + \alpha^2} \cos[\nu(\mathbf{k}; t)]; \\ \hat{v}_z(\mathbf{k}; t) &= \frac{1}{A(\omega^2 + \alpha^2)^{3/4}} \int_0^t dt \frac{\hat{h}_1(t)}{(\omega + \alpha^2)^{1/4}} \cos[\nu(\mathbf{k}; t)] + \frac{\omega}{\omega^2 + \alpha^2} \sin[\nu(\mathbf{k}; t)] \\ &\quad + \hat{h}_2(t) (\omega + \alpha^2)^{1/4} \sin[\nu(\mathbf{k}; t)] + \frac{\omega}{\omega^2 + \alpha^2} \cos[\nu(\mathbf{k}; t)]. \end{aligned} \quad (21)$$

Here,

$$\begin{aligned} \omega &= \omega_j; \quad \alpha = \alpha_j; \quad \nu = \text{sign}(\omega_j); \\ s(t) &= 1 - \frac{1}{2} \text{arcsinh} \frac{t}{\omega} + O\left(\frac{1}{\omega}\right); \\ \nu(\mathbf{k}; t) &= \nu_0 [s(t) - s(\mathbf{k})]: \end{aligned} \quad (22)$$

In the following subsections, we compute the various correlation functions by assuming a homogeneous and short-correlated forcing [see equation (11)]. As the system (16) involves the forcing in terms of \hat{h}_1 and \hat{h}_2 only [see equation (17)], we define the power spectrum $\langle \hat{v}_i \hat{v}_j \rangle$ as:

$$\langle \hat{v}_i(\mathbf{k}_1; t_1) \hat{v}_j(\mathbf{k}_2; t_2) \rangle = \frac{1}{(2\pi)^3} \delta(\mathbf{k}_1 + \mathbf{k}_2) \delta(t_1 - t_2) \langle \hat{v}_i(\mathbf{k}_2) \rangle; \quad (23)$$

for i and $j = 1$ or 2 . In the case of an isotropic and incompressible forcing [equation (12)], $\langle \hat{v}_i \hat{v}_j \rangle$ in equation (23) can be written:

$$\langle \hat{v}_1 \hat{v}_1 \rangle(\mathbf{k}) = (\omega^2 + \alpha^2) F(\mathbf{k}); \quad \langle \hat{v}_2 \hat{v}_2 \rangle(\mathbf{k}) = 0; \quad \langle \hat{v}_1 \hat{v}_2 \rangle(\mathbf{k}) = F(\mathbf{k}); \quad (24)$$

3.1.1 Turbulence intensity

Using equations (21) and (23), we obtain the following turbulence intensity in the x direction:

$$\begin{aligned} \langle \hat{v}_x^2 \rangle &= \frac{1}{(2\pi)^3 A} \int d^3k \int_0^t dt \frac{e^{2Q(\mathbf{k}) - Q(\mathbf{a})} \omega^{2n}}{(\omega^2 + \alpha^2)^{3/2}} \left[\frac{11(\mathbf{k})}{\omega^2 + \alpha^2} \cos^2[\nu(\mathbf{a}; t)] \right. \\ &\quad \left. + \frac{12(\mathbf{k}) \sin[2\nu(\mathbf{a}; t)] + 22(\mathbf{k}) \frac{\omega}{\omega^2 + \alpha^2} \sin^2[\nu(\mathbf{a}; t)] \right]; \end{aligned} \quad (25)$$

Here, $\mathbf{a} = k_x = k_y$, $\omega = k_z = k_y$, $\nu = 1 + \alpha^2$, $\omega = A = (\frac{k^2}{\nu})$ and $Q(\mathbf{x}) = x^3 = 3 + x$. In the case of an isotropic forcing [equation (24)], equation (25) and the turbulence

intensity in the two other directions can then be derived as:

$$\begin{aligned} \overline{w_x^2} &= \frac{f}{(2\pi)^3 A} \int_0^Z d^3k \frac{F(k)}{k^2 + a^2} I^0(k); \\ \overline{w_y^2} &= \frac{f}{(2\pi)^3 A} \int_0^Z d^3k \frac{F(k)}{k^2 + a^2} (I^0(k) + I^2(k)); \\ \overline{w_z^2} &= \frac{f}{(2\pi)^3 A} \int_0^Z d^3k \frac{F(k)}{k^2 + a^2} (I^0(k) + I^2(k)). \end{aligned} \quad (26)$$

Here:

$$I^p(k) = \int_0^Z \frac{e^{-2Q(z)} Q^p(a)}{(k^2 + a^2)^{3/2}} dz \quad (27)$$

In order to elucidate the effect of shear flow on rotating turbulence, we estimate the integral I_p in equation (27) in the weak ($k^2 = A^{-1}$) and strong ($k^2 = 1$) shear limits.

First, in the weak shear limit ($k^2 = 1$), the integral I_p in equation (27) takes the approximate value:

$$I^p(k) \approx \frac{a^p}{2(k^2 + a^2)^{3/2}} = \frac{A a^p}{2 k^2 (k^2 + a^2)^{3/2}} \quad (28)$$

By using equation (28) in equation (26), we can then obtain the following result for the turbulent intensity:

$$\begin{aligned} \overline{w_x^2} &= \frac{f}{(2\pi)^3} \int_0^Z d^3k \frac{F(k)}{2 k^2 (k^2 + a^2)}; \\ \overline{w_y^2} &= \frac{f}{(2\pi)^3} \int_0^Z d^3k \frac{F(k)}{2 k^2 (k^2 + a^2)} (1 + a^2/k^2); \\ \overline{w_z^2} &= \frac{f}{(2\pi)^3} \int_0^Z d^3k \frac{F(k)}{2 k^2 (k^2 + a^2)} (1 + a^2/k^2). \end{aligned} \quad (29)$$

Performing the integration over the angular variable, we obtain:

$$\begin{aligned} \overline{w_x^2} &= \frac{f}{(2\pi)^3} \int_0^Z dk \frac{F(k)}{2} \int_0^{\pi/2} \int_0^{2\pi} d\theta \sin^2 \theta \cos^2 \theta + \int_0^{\pi/2} \int_0^{2\pi} d\theta \sin^2 \theta \sin^2 \theta \\ &= \frac{2f}{3(2\pi)^2} \int_0^Z dk \frac{F(k)}{2}; \end{aligned} \quad (30)$$

and exactly the same expression for the turbulence intensity in the other two directions. These results indicate that, in the large rotation limit, the turbulence intensity is isotropic and equals to the one without rotation [see equation (13)]. This result is consistent with the result of Cambon et al. (1997) which showed that the anisotropy in rotating flows was induced by non-linear interactions and thus cannot be captured by a linear theory such as the one we used. However, in the presence of strong shear flows, the velocity amplitude is no longer isotropic, as shown below.

Second, in the strong shear limit ($k^2 = 1$), the integral (27) take the following form

$$\begin{aligned} I^0(k) &= \frac{1}{2} \int_0^Z \frac{a}{k^2 + a^2} dz; \\ I^2(k) &= \frac{\ln}{3} \quad (31) \end{aligned}$$

By plugging equation (31) in equation (26), we obtain:

$$\begin{aligned} \overline{v_x^2} &= \frac{f}{(2\pi)^3 A} \int d^3k \frac{P}{\omega^2 + \alpha^2 F(k)} ; \\ \overline{v_y^2} &= \frac{f}{(2\pi)^3 A} \int d^3k \frac{P}{\omega^2 + \alpha^2 F(k)} \frac{\ln}{3} ; \\ \overline{v_z^2} &= \frac{f}{(2\pi)^3 A} \int d^3k \frac{P}{\omega^2 + \alpha^2 F(k)} \frac{\ln}{3} ; \end{aligned} \quad (32)$$

to leading order in α . Note that in the calculation of $\overline{v_x^2}$, we neglected the component proportional to $\alpha = k_x = k_y$ as it is odd in both k_x and k_y and thus vanishes after integration over the angular variables. Equation (32) shows that the turbulence intensity is reduced due to the shear A but effectively stronger in the x direction than in the perpendicular one, by a factor of \ln . This shows that shear flow can induce anisotropic turbulence (unlike rotation) even when the forcing is isotropic. This result agrees with the simulation of a Couette flow at high rotation rate (Bech & Andersson, 1997) where the velocity fluctuations perpendicular to the wall exceed that in the streamwise direction. Furthermore, rapid rotation results in $\overline{v_y^2} = \overline{v_z^2}$ with the same velocity fluctuations in the y and z directions. This contrasts to the case of slow rotation (considered in §3.2) where $\overline{v_y^2}$ is larger than $\overline{v_z^2}$.

3.1.2 Transport of angular momentum

In the case of an isotropic forcing, we obtain the following Reynolds stress from equations (21) and (23):

$$\overline{v_x v_y} = \frac{f}{(2\pi)^3 A} \int d^3k \frac{P}{\omega^2 + \alpha^2 F(k)} I^1(k) ; \quad (33)$$

where I^1 was defined in equation (27). In the following, we again consider the weak and strong shear limits.

First, in the weak shear limit ($\alpha \ll 1$), there is no contribution to leading order as the function I^1 is odd in α and thus vanishes after integration over the wave vector. We thus include one higher order in the expansion and obtain the following result:

$$\overline{v_x v_y} = \frac{f}{(2\pi)^3 A} \int d^3k \frac{\alpha F(k)}{2\omega_0} J(k) ; \quad (34)$$

Here, we defined a function $J(k)$, which has the following asymptotic behaviour in the weak shear limit:

$$J(k) = \frac{\int_0^{\alpha} e^{-2Q(\cdot)Q(a)} \sin[2!_0 fs(a) - s(\cdot)g] d}{\frac{\alpha \overline{\omega_0} A}{2(\omega^2 + \alpha^2)^{3/2} [2k^4 + \overline{\omega_0}^2]}} ; \quad (35)$$

where $\overline{\omega_0} = \omega_0 A = \int_0^{\alpha} \frac{P}{\omega^2 + \alpha^2}$. Plugging equation (35) in equation (34) and performing the integration over the azimuthal angle variable ϕ , we obtain:

$$\overline{v_x v_y} = \frac{f A}{32(3\pi)^2} \int_0^{\alpha} dk k^2 F(k) \int_0^{\alpha} d \sin^5 \frac{1}{2k^4 + \overline{\omega_0}^2} ; \quad (36)$$

Finally, we change the integration variable from θ to $T_0 = \cos \theta$, obtaining the following formula:

$$\langle w_x v_y \rangle = \frac{\epsilon A}{16(2j)^2} \int_0^Z dk k^2 F(k) \int_0^Z dT_0 \frac{1 - T_0^2}{2k^4 + T_0^2} : \quad (37)$$

Therefore, in the large rotation and weak shear limit, the Reynolds stress becomes purely dispersive (with no effect) with the following turbulent viscosity:

$$\tau = \frac{\epsilon}{32(2j)^2} \int_0^Z dk \frac{F(k)}{k^2} : \quad (38)$$

This result shows that the turbulent viscosity is positive and proportional to $\epsilon^{1/2}$ for large j . It is worth comparing equation (38) with equation (22) in Kichatinov (1986). To this end, we use equation (13), which gives the turbulence amplitude without rotation (the original turbulence of Kichatinov) in equation (38) to obtain the turbulent viscosity $\tau = \frac{1}{2} \epsilon^{1/2} = 64j^2$. Thus τ in equation (38) is the same as equation (22) in Kichatinov (1986) for $j \gg 1$ and $\Omega = \Omega_0$, but has an opposite sign. In other words, we obtain $\tau > 0$ whereas Kichatinov (1986) obtained $\tau < 0$.

In comparison, in the strong shear limit (equation 1), the function I^1 in equation (27) has the following asymptotic behaviour for $j \gg 1$:

$$I^1(k) = \frac{1}{k^2 + a^2} : \quad (39)$$

Plugging equation (39) in equation (33), we obtain the turbulent viscosity in the strong shear limit as:

$$\tau = \frac{\langle w_x v_y \rangle}{A} = \frac{\epsilon}{(2j)^3 A^2} \int_0^Z dk^3 F(k) : \quad (40)$$

Equation (40) shows that the turbulent viscosity is negative (as $F(k) > 0$) in the strong shear limit, in sharp contrast to the weak shear limit where $\tau > 0$ [see equation (38)]. Furthermore, the magnitude of τ is reduced only by the shear ($\propto A^{-2}$) and is independent of rotation, which should also be compared to the weak shear limit [see equation (38) where $\tau \propto \Omega^{1/2}$]. Therefore, the turbulent viscosity changes from positive (for weak shear) to negative (for large shear) as the ratio of shear to dissipation increases. This result can be understood if we assume that, as in most rapidly rotating fluid, the inverse cascade is associated with the conservation of a potential vorticity (Pedlovsky, 1987). In presence of strong shear (compared to dissipation), the potential vorticity is strictly conserved giving rise to an inverse cascade (negative viscosity). When the dissipation increases, the potential vorticity is less and less conserved and thus the inverse cascade is quenched. Our results show that there is a transition from inverse to direct cascade as the dissipation is increased. A similar behaviour is also found in two-dimensional hydrodynamics (HD) where an inverse cascade can be shown to be present only for sufficient weak dissipation (Kim & Dubrulle, 2001).

The preceding results [equation (38) and (40)] indicate that in the large rotation limit where rotation dominates over shear, the momentum transport

is purely dissipative for isotropic forcing, with opposite sign of turbulent viscosity for weak (1) and strong shear (1) for a fixed value of $j \neq A$ (1). In the case of anisotropic forcing, there is however a possibility of the appearance of non-dissipative momentum transport (effect). To examine this possibility, we now consider an extremely anisotropic forcing (introduced in x2.3) where the forcing is restricted to horizontal plane (y-z), perpendicular to the direction of the shear. Using equation (14) with $g_{ij} = \delta_{ij}$, we obtain the following Reynolds stress:

$$\overline{u_x v_y} = \frac{f}{(2A)^3} \int d^3k \frac{G(k)}{2(\omega^2 + \alpha^2)} \left[I^1(k) - J^0(k) + K(k) \right] \quad (41)$$

Here, I^1 was defined previously in equation (27) and:

$$J^0(k) = \int_a^{Z+1} \frac{e^{-2Q(\cdot)Q(a)}}{(\omega^2 + \alpha^2)^{3/2}} \cos[2!_0 fs(a) - s(\cdot)g] d \quad ; \quad (42)$$

$$K(k) = \int_a^{Z+1} \frac{e^{-2Q(\cdot)Q(a)}}{(\omega^2 + \alpha^2)} \sin[2!_0 fs(a) - s(\cdot)g] d \quad ;$$

We again consider the weak and strong shear limits in the following. First, in the weak shear limit (1), equation (41) is simplified to:

$$\overline{u_x v_y} = \frac{f}{(2A)^3} \int d^3k \frac{G(k)}{4(\omega^2 + \alpha^2)^{3/2}} \frac{\overline{\Gamma_0}}{2k^4 + \overline{\Gamma_0}^2} \quad (43)$$

Performing the angular integration in equation (43) and taking the large rotation limit, we obtain the following:

$$\overline{u_x v_y} = \frac{f}{3(2A)^3} \int d^3k \frac{G(k)}{A} \quad (44)$$

Equation (44) is odd in the rotation and thus represents the effect. Again, the latter favours the creation of velocity gradient rather than smoothing it out and can thus provide a mechanism for the occurrence of differential rotation (e.g. in the sun). By using equation (15), one can see that the effect is proportional to the anisotropy in the turbulence without shear and rotation. This result shows that, in the large rotation limit, one needs anisotropic forcing to generate non-dissipative vortices of angular momentum (as in the case without shear as shown Kichatinov, 1986). This should be contrasted to the case of weak rotation (x3.2) where the shear can alone give rise to an anisotropic turbulence, thereby leading to a effect even with an isotropic forcing.

Finally, in the strong shear limit, equation (41) becomes:

$$\overline{u_x v_y} = \frac{f}{(2A)^3} \int d^3k \frac{G(k)}{2(\omega^2 + \alpha^2)} \quad ; \quad (45)$$

which is even in the rotation. Thus, the turbulent viscosity τ is obviously positive. Thus, in the large shear limit (but still negligible compared to the rotation), anisotropic forcing does not induce any non-dissipative vortices but just increases the magnitude of the negative turbulent viscosity.

3.1.3 Transport of particles

In this section, we show that in the large rotation limit ($j \gg A^{-1}$), the transport of particles is mainly governed, to leading order, by rotation. By using equations (10), (21) and (23) and going through a similar long, but straightforward analysis as previously, we can obtain the turbulent diffusivities of chemicals:

$$D_T^{xx} = \frac{f}{(2j)^3 A^2} \int d^3k \frac{F(k)}{(\omega + a^2)^{1=4}} \frac{S_3^0}{\omega_0}; \quad (46)$$

$$D_T^{yy} = \frac{f}{(2j)^3 A^2} \int d^3k \frac{P}{\omega_0} \left[\frac{aS_3^1}{(\omega + a^2)^{1=4}} + \frac{P}{(\omega + a^2)^{1=4}} \frac{a^2 C_3^1}{\omega_0} + \frac{a C_1^0}{\omega_0} \frac{2}{(\omega + a^2)^{1=4}} S_1^0 + \frac{2P}{2(\omega + a^2)^{3=4}} + \frac{a^2 C_1^0}{\omega_0} a C_3^1 + \frac{2}{2(\omega + a^2)^{3=4}} a S_1^0 + \frac{P}{\omega_0} \frac{a^2 S_3^1}{\omega_0} \right];$$

where:

$$P_n^p(k) = \frac{\int_0^{Z+1} P e^{-2Q(\cdot)Q(a)} (\omega + a^2)^{n=4} \exp[i\omega_0 fs(a) - s(\cdot)g] d\cdot; \quad (47)$$

$$P_n^p(k) = \frac{\int_0^{Z+1} P e^{-2Q(\cdot)Q(a)} (\omega + a^2)^{n=4} (\omega_0 - a) \exp[i\omega_0 fs(a) - s(\cdot)g] d\cdot;$$

$$C_n^p = \langle P_n^p \rangle; \quad S_n^p = \langle P_n^p \rangle; \quad C_n^p = \langle P_n^p \rangle; \quad S_n^p = \langle P_n^p \rangle;$$

The expression for D_T^{zz} is omitted here as it is very similar of that for D_T^{yy} . To compute the asymptotic behaviour of integrals (47), the distinction between large and weak shear is not necessary as, for $\omega_0 \gg 1$, these integrals can easily be evaluated to leading order as:

$$P_n^p(k) = \frac{a^p (2k^2 - \overline{\omega_0}) A}{(\omega + a^2)^{n=4} [4k^4 + \overline{\omega_0}^2]}; \quad (48)$$

where $\overline{\omega_0} = \omega_0 A = \frac{P}{\omega + a^2}$. In comparison, the functions P_n^p vanish to leading order and are thus omitted here. By using equation (48) in equation (46), we obtain the following results:

$$D_T^{xx} = \frac{f}{(2j)^3} \int d^3k F(k) \frac{1}{\omega + a^2} \frac{1}{4k^4 + \overline{\omega_0}^2}; \quad (49)$$

$$D_T^{yy} = \frac{f}{(2j)^3} \int d^3k F(k) \frac{a^2 + \omega^2}{(\omega + a^2)} \frac{1}{4k^4 + \overline{\omega_0}^2};$$

$$D_T^{zz} = \frac{f}{(2j)^3} \int d^3k F(k) \frac{1 + a^2}{(\omega + a^2)} \frac{1}{4k^4 + \overline{\omega_0}^2};$$

Here, we have discarded all the terms which are odd in a (for example in D_T^{yy} , the terms proportional to C_1 and C_3) as they vanish after angular integration, which gives the following result:

$$D_T^{xx} = \frac{f}{8jj} \int_0^Z \frac{F(k)}{k} dk; \quad (50)$$

$$D_T^{yy} = D_T^{zz} = \frac{f}{16jj} \int_0^Z \frac{F(k)}{k} dk;$$

Equation (50) shows that D_T^{xx} , D_T^{yy} and D_T^{zz} are all reduced as Ω^{-1} for large Ω and also that there is only a slight anisotropy in the transport of scalar: the transport in the direction of the rotation is twice larger than the one in the perpendicular direction (Kichatinov et al., 1994). This anisotropy is present in the transport of particles but not in the turbulence intensity [see equation (30)] because rotation affects only the phase between the different velocity components and not their magnitude. Note also that this anisotropy is much weaker than that in sheared turbulence without rotation (Kim, 2005).

To summarise, this section shows how a shear flow can affect the turbulent transport when turbulence is largely dominated by rapid rotation ($\Omega \gg \Lambda^{-1}$). In particular, the results indicate that shear flow can induce a strong anisotropic turbulence [equation (32)] (with an effectively weaker turbulence in the direction of the shear), which would otherwise be almost isotropic [equation (29)].

3.2 Weak rotation limit: $\Omega \ll \Lambda^{-1}$

In this section, we consider the case when shear dominates over rotation ($\Omega \ll \Lambda^{-1}$) to study how the rotation alters the transport properties in the sheared turbulence (studied in Kim, 2005). In the weak rotation limit, we expand quantities in powers of $\Omega = \Omega \Lambda^{-1}$ as:

$$X(\mathbf{x}) = X_0(\mathbf{x}) + \Omega X_1(\mathbf{x}) + \dots; \quad (51)$$

and calculate the turbulence intensity and transport up to first order in Ω . For the sake of brevity, we here just provide the final results of the calculation.

3.2.1 Turbulence intensity

By using the expansion in powers of Ω and equation (23) and after a long, but straightforward algebra, we can obtain the turbulence intensity in the x direction as follows:

$$\overline{v_x^2} = \frac{f}{(2\pi)^3 \Lambda^3} \int d^3k \left[L_0(k) + \Omega L_1(k) \right]; \quad (52)$$

Here:

$$L_0(k) = \int_{-Z}^{Z+1} d\alpha \frac{e^{-2\alpha} [Q(\alpha) - Q(a)]}{(\alpha^2 + a^2)^2}; \quad (53)$$

$$L_1(k) = \int_a^{Z+1} d\alpha \frac{e^{-2\alpha} [Q(\alpha) - Q(a)]}{(\alpha^2 + a^2)^2} fT(\alpha) - T(a)g \frac{1}{2} \ln \frac{\alpha^2 + a^2}{a^2};$$

$$T(x) = \frac{1}{\pi} \arctan \frac{x}{a};$$

In the strong shear limit ($\Omega \ll 1$), the integrals L_0 and L_1 in equation (53) can be simplified:

$$L_0(k) = \int_{-Z}^{Z+1} d\alpha \frac{1}{(\alpha^2 + a^2)^2} = \frac{1}{2} \frac{1}{a^2} T(a) \frac{a}{a^2}; \quad (54)$$

$$L_1(k) = \int_a^{Z+1} d\alpha \frac{1}{(\alpha^2 + a^2)^2} fT(\alpha) - T(a)g \frac{1}{2} \ln \frac{\alpha^2 + a^2}{a^2}$$

$$= \frac{1}{2(\alpha^2 + a^2)} + \frac{1}{2} T(\alpha) fT(\alpha) - T(a)gd;$$

Note that the second formula for L_1 in equation (54) was obtained by integration by part. Equation (54) clearly shows that L_1 is positive for all values of a (for $a < 0$, the negative part of the integral is always smaller than the positive one as the first term is odd in k_x and the second one is an increasing function of a). Therefore, the turbulence intensity $\langle v_x^2 \rangle$ in equation (52) increases for $a > 0$ whereas it decreases for $a < 0$. This can be understood from figure 2 which shows that the homogeneous solution decays faster as the parameter b is increased (recall that $b = a^2$ in the weak shear limit). Therefore, we recover the conclusion of the stability analysis performed at the beginning of §3: a weak rotation destabilises sheared turbulence for $a > 0$ whereas it stabilises for $a < 0$.

Performing similar calculations for the other components of the turbulence amplitude, we obtain the following result in the strong shear limit (1):

$$\langle v_y^2 \rangle = \frac{f}{(2\pi)^3 A} \int d^3 k \frac{1}{2^p} T(a) \left[\Gamma(1+3) + \Gamma(4+3) \left(\ln \frac{1}{k} \right) \right] \left[\Gamma(1+3) + \Gamma(4+3) \left(\ln \frac{1}{k} \right) \right] \quad (55)$$

$$\langle v_z^2 \rangle = \frac{f}{(2\pi)^3 A} \int d^3 k \frac{1}{2^p} T(a) \left[\Gamma(1+3) + \Gamma(4+3) \left(\ln \frac{1}{k} \right) \right] \left[\Gamma(1+3) + \Gamma(4+3) \left(\ln \frac{1}{k} \right) \right]$$

Here, Γ is the Gamma function. Equation (55) shows that, here again, the turbulence amplitude is increased or decreased due to the weak rotation depending on the sign of a . Furthermore, the correction now has a logarithmic dependence on the shear, contrary to the case of the amplitude in the shear (x) direction, which is independent of shear [equation (52)]. Therefore, the turbulence in the $y-z$ plane is more affected by rotation than the one in the x direction. As a result, the turbulence due to shearing becomes less anisotropic. This illustrates the tendency of rotation to lead to almost isotropic turbulence. The results for $\langle v_y^2 \rangle$ and $\langle v_z^2 \rangle$ are very similar but, as k_y and k_z do not play symmetric roles, not exactly the same. For an isotropic forcing, the angular integration gives that $\langle v_y^2 \rangle$ is larger than $\langle v_z^2 \rangle$. This effect appears at leading order and is thus only an effect of the shear that has already been evidenced by numerical simulations: the fluctuating velocity in the direction of the flow is larger than the one in the direction of the shear (Lee et al., 1990). This should be contrasted to the result (32) in the case of rapid rotation, where we showed that the turbulence in the $y-z$ plane was isotropic ($\langle v_y^2 \rangle = \langle v_z^2 \rangle$). This clearly illustrates the tendency of rotation to make almost isotropic turbulence.

In summary, in the case of a strong shear turbulence ($A \gg \lambda_j$ and $A \gg k_y^2$), the rotation can either enhance or reduce the turbulence amplitude, depending on the relative sign of the rotation a and shear A , and tends to reduce the anisotropy in sheared turbulence.

3.2.2 Transport of angular momentum

In the strong shear limit (1), the transport of angular momentum can be derived as:

$$\begin{aligned} \langle v_x v_y \rangle &= \frac{f}{(2\pi)^3 A} \int d^3 k \frac{\langle \tau_{11}(k) \rangle}{2(\omega + a^2)} + \frac{2}{2\pi} \langle \tau_{11}(k) \rangle + \frac{2}{3} \langle \tau_{22}(k) \rangle \ln \left(\frac{\omega + a^2}{\omega} \right) \end{aligned} \quad (56)$$

For $\omega = 0$, we recover the result of Kim (2005) that the turbulent viscosity is reduced proportionally to A^{-2} for strong shear. The correction due to the rotation is proportional to Ω and is odd in the rotation. This is the so-called Coriolis effect, a non-dissipative contribution to Reynolds stress. It is important to emphasise that non-trivial Coriolis effect results from an anisotropy induced by shear flow on the turbulence even when the driving force is isotropic. This should be contrasted to the case without shear flow where non-dissipative fluxes emerge only for anisotropic forcing. A similar result was also found in §3.1.2 [see equations (38) and (40)]. This Coriolis effect [the second term in equation (56)] is obviously of the same sign as Ω whereas the turbulent viscosity [the first term in equation (56)] can either be positive or negative, depending on the relative magnitude of the two terms inside the integral. In the two-dimensional limit or for a symmetric perturbation with $k_z = 0$ ($\Omega = 0$), we can easily show that the turbulent viscosity is negative. On the contrary, in the case of an isotropic forcing in three-dimensional, the turbulent viscosity is positive. This is in agreement with previous studies which showed that non-dissipative fluxes of angular momentum (Rudiger, 1980; Kichatinov, 1986) are proportional to the anisotropy in the background turbulence. However, in our case, the anisotropy is not artificially introduced in the system but is created by the shear and calculated self-consistently.

3.2.3 Transport of particles

In the strong shear limit (1), we can compute the transport of particles $\langle v_x v_x \rangle$ with the result:

$$\begin{aligned} D_T^{xx} &= \frac{f}{(2\pi)^3 A^2} \int d^3 k \frac{\langle \tau_{11}(k) \rangle}{2\pi} \langle \tau_{11}(k) \rangle + \frac{2}{3} \langle \tau_{22}(k) \rangle \ln \left(\frac{\omega + a^2}{\omega} \right) ; \quad (57) \\ D_T^{zz} &= \frac{f}{(2\pi)^3 A^2} \int d^3 k \frac{\langle \tau_{11}(k) \rangle^2}{2} \langle \tau_{11}(k) \rangle + \frac{2\langle \tau_{22}(k) \rangle}{2} \\ &= \frac{1}{3} \frac{3}{2} \langle \tau_{11}(k) \rangle^2 + \frac{2}{3} \langle \tau_{22}(k) \rangle \ln \left(\frac{\omega + a^2}{\omega} \right) \end{aligned}$$

Equation (57) shows that the effect of rotation on the transport of particles depends on the sign of Ω : for $\Omega > 0$, the transport is increased whereas it is reduced for $\Omega < 0$. Again, this is because a weak rotation destabilises sheared turbulence for $\Omega > 0$ whereas it stabilises for $\Omega < 0$ (see figure 3 and the discussion at the beginning of §3). Note that a similar behaviour was also found in turbulence intensity, given in equations (52) and (55). The correction term

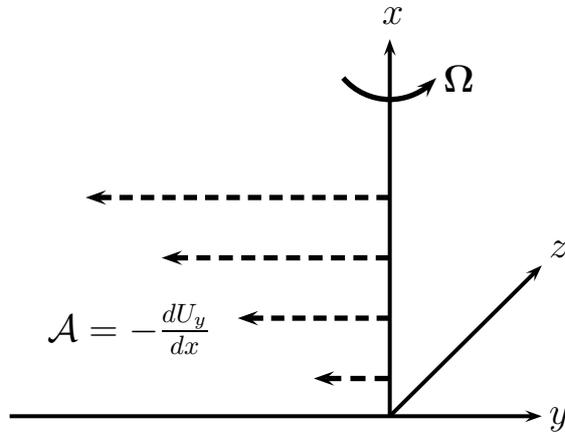


Figure 4: Sketch of the configuration in the parallel case

due to rotation in D_T^{xx} and D_T^{zz} in equation (57) depends weakly on the shear by a logarithmic factor $|\ln \lambda|$, which cannot be too large even for $\lambda = \frac{z}{y} = A^{-1}$, and is of the same order for transport in different directions. Thus, the scaling of the turbulent diffusivity is roughly the same as in the case without rotation: the transport in x direction is more reduced (by a factor A^{-2}) than the one in the $y-z$ plane (by a factor $A^{-4=3}$). This result should be contrasted to the large rotation case where the transport in the shear (x) direction was larger (by a factor 2) than the one in the perpendicular direction. These results highlight the crucial role of shear in transport, in particular in introducing anisotropy.

To summarise, in the slow rotation limit, where turbulence is mainly regulated by shear flow, the turbulence intensity [equations (52) and (55)] and transport [equation (57)] are shown to be strongly anisotropic due to shear flow while they are slightly enhanced or reduced by rotation for $\Omega > 0$ or $\Omega < 0$, respectively, to next order. The strong anisotropic turbulence was shown to give rise to a defect for momentum transport [equation (56)] even for an isotropic forcing.

4 The parallel case ($\Omega = 0$)

We now study the case where the shear and the rotation are parallel as depicted in figure 4. Setting $\Omega = 0$ and rearranging (5) in order to eliminate the pressure terms, the three remaining equations can be written:

$$\begin{aligned} \partial_t \hat{h}_1 + \partial_x \hat{f} + \partial_x^2 \hat{v}_x + (\partial_x^2 - \partial_x) \hat{v}_x &= \partial_x \frac{\hat{h}_1(\cdot)}{A} - \frac{\hat{h}_2(\cdot)}{A}; \quad (58) \\ \partial_t \hat{v}_z &= -\partial_x \hat{v}_x + \frac{\hat{h}_2(\cdot)}{A}; \\ \hat{v}_y &= (\hat{v}_x + \hat{v}_z): \end{aligned}$$

Here again, $k_z = k_y$, $\omega = 1 + \omega^2 = k_H^2 = k_y^2$ and $\omega = \omega A$. We first study the stability of the homogeneous solution in the long time limit. Setting $\hat{h}_1 = \hat{h}_2 = 0$ in the first equation of (58), the long time behaviour (for $j = j$) is given by:

$$\partial_t \frac{h_1}{\omega} + \omega^2 g \hat{v}_x + \omega^2 \hat{v}_x = 0 : \quad (59)$$

Making the change of variable $x = \frac{p}{\omega + \omega^2}$ and letting $\hat{v}_x(\omega) = h(x) = x$, the equation for h becomes

$$x^2 h''(x) + x h'(x) + (\omega^2 x^2 - 1) h(x) = 0 : \quad (60)$$

Two independent solutions to equation (60) are given by a Bessel function of the first kind $J_1(j \sqrt{x})$ and of the second kind $Y_1(j \sqrt{x})$. Thus, the general solution of equation (59) can be written as:

$$\hat{v}_x(\omega) = \frac{1}{\omega + \omega^2} \left[A J_1(j \sqrt{\frac{p}{\omega + \omega^2}}) + B Y_1(j \sqrt{\frac{p}{\omega + \omega^2}}) \right] ; \quad (61)$$

for large time. It is then easy to see that $\hat{v}_x(\omega) \rightarrow 0$ as $\omega \rightarrow +1$. We can also show (see Appendix A for details) that the other two components of the velocity vanish for large time. Consequently, the configuration is always linearly stable. Furthermore there is no effect at all of rotation on the stability of shear flows in this configuration.

To calculate the turbulence amplitude and transport, the first equation in equation (58) is to be solved with initial conditions: $\hat{v}_x(\omega_0) = 0$ and $\partial_t \hat{v}_x|_{\omega=\omega_0} = h_1(\omega_0) = (\omega_0 + \omega_0^2) A$. Unfortunately, we were unable to find an exact solution of equation (58) in the general case. Thus, to gain a useful insight into the problem, we here focus on the three simplified cases where approximate solutions can be found: the large rotation limit in x4.1 where we find a WKB solution of equation (58), the weak rotation limit in x4.2 and finally, in x4.3, we consider the symmetric perturbation (with $\omega = 0$) to find an exact solution. As the results of the two first sections are very similar to the perpendicular case (x3), we here just show the differences because of the different configuration of shear and rotation.

4.1 Large rotation limit: $j \gg 1$ (and $a > 0$)

For $j \gg 1$, we seek for a WKB solution of the first equation in equation (58). However, since this approximation breaks for $\omega = 0$, we assume that the initial value is positive ($\omega_0 = a > 0$) to make our solution meaningful. In x4.3, we study an exactly solvable case and show that the solution can be altered by negative initial value ($\omega_0 = a < 0$). Assuming $\omega_0 = a > 0$, we obtain the following

solutions for the three components of the velocity for $j = A j - 1$:

$$\begin{aligned}
 \hat{v}_x(t) &= \frac{1}{A(\epsilon^2)^{3/4}} \int_0^Z dt \frac{\hat{h}_1(t)}{(\epsilon^2)^{1/4}} \cos[v(t; \epsilon)] + \hat{h}_2(t) (\epsilon^2)^{1/4} \sin[v(t; \epsilon)] ; \\
 \hat{v}_y(t) &= \frac{1}{A(\epsilon^2)^{3/4}} \int_0^Z dt \frac{\hat{h}_1(t)}{(\epsilon^2)^{1/4}} \cos[v(t; \epsilon)] + \frac{p}{\epsilon^2} \sin[v(t; \epsilon)] \\
 &\quad + \hat{h}_2(t) (\epsilon^2)^{1/4} \sin[v(t; \epsilon)] \frac{p}{\epsilon^2} \cos[v(t; \epsilon)] ; \\
 \hat{v}_z(t) &= \frac{1}{A(\epsilon^2)^{3/4}} \int_0^Z dt \frac{\hat{h}_1(t)}{(\epsilon^2)^{1/4}} \cos[v(t; \epsilon)] \frac{p}{\epsilon^2} \sin[v(t; \epsilon)] \\
 &\quad + \hat{h}_2(t) (\epsilon^2)^{1/4} \sin[v(t; \epsilon)] \frac{p}{\epsilon^2} \cos[v(t; \epsilon)] :
 \end{aligned} \tag{62}$$

Here,

$$\begin{aligned}
 \epsilon_0 &= |j| ; \quad \epsilon = \text{sign}(\epsilon) ; \\
 r(t) &= \frac{p}{\epsilon^2} \frac{h}{2} \ln \frac{h}{\epsilon_0} + \frac{p}{\epsilon^2} i + O\left(\frac{1}{\epsilon_0}\right) ; \\
 v(t; \epsilon) &= \epsilon_0 [r(t) - r(\epsilon)] :
 \end{aligned} \tag{63}$$

Due to the similarity between equation (62) and equation (21) obtained in the perpendicular case in §3.1, the turbulence amplitude can easily be shown to be the same as that of equation (26). Similarly, the turbulent viscosity is the same as previously [see equation (33)] with a negative eddy-viscosity in the strong shear limit. In the weak shear limit, however, the next order term is odd in ϵ and thus vanishes for an isotropic forcing, giving no contribution to the eddy-viscosity. Consequently, the eddy viscosity vanishes to leading order (for rotation and shear parallel) in the weak shear limit. Also, the transport of particles is the same as previously [see equation (50)] both in the strong and weak shear limit.

4.2 Weak rotation limit: $A \ll 1$

In the weak rotation limit, we expand all the quantities in powers of ϵ_0 as:

$$X(\epsilon) = X_0(\epsilon) + \epsilon_0 X_1(\epsilon) + \dots \tag{64}$$

Contrary to the perpendicular case, we find that the leading order correction (proportional to ϵ_0) vanishes in the case of an isotropic forcing (because these terms are odd in ϵ) for all the previously calculated quantities. However, the component of the Reynolds stress involving the velocity component v_z does not vanish and is odd in ϵ . Thus, the ϵ -effect appears here in the other component of the Reynolds stress τ_z (recall that in the perpendicular case, the ϵ -effect was present only in $\langle v_x v_y \rangle$), in the form:

$$\tau_z = \frac{f}{(2\epsilon)^3 A^2} \int d^3 k \frac{(2=3)}{6^2} \frac{3}{2} \epsilon^{2=3} (3^2 - 1) \epsilon^2 \frac{p}{2} = T(a) \tau_{11}(k) + \tau_{22}(k) : \tag{65}$$

Equation (65) shows that the sign of τ_z is indefinite (as both signs appear in the prefactor $(3^2 - 1)$). However, as for equation (56), in the case of an isotropic

forcing, the term proportional to ω^2 dominates, making ω_z negative. This effect appears due to the anisotropy between the y - and the z -components of the velocity, due to the shear (alone) as shown in x3.2.1

4.3 Symmetric perturbation ($\omega = 0$)

In this section, we consider a symmetric perturbation with $k_z = 0$ by assuming a forcing that is symmetric in the z direction. For $\omega = k_z = k_y = 0$, the homogeneous part of the first equation in (58) becomes:

$$\partial_t \left[\frac{h_1}{2} \partial_z (1 + \omega^2 \hat{v}_x) + \frac{h_2}{2} \hat{v}_z \right] = 0 : \quad (66)$$

This equation is the same as the one we obtained for the study of the stability of the configuration where the shear and the rotation are parallel [see equation (59) with $\omega = 1$]. Solutions of the homogeneous problem are thus Bessel functions. Using the method of variation of parameters, we can then express the general solution of the first equation to (58) as:

$$\hat{v}_x(z) = \frac{h_1}{2} \int_0^z \frac{dt}{1 + \omega^2 t^2} L_{01}(t; \omega) + \frac{h_2}{A} \int_0^z \frac{dt}{1 + \omega^2 t^2} L_{11}(t; \omega) : (67)$$

Here again, $\omega = |\mathbf{j}|$, $\omega = \text{sign}(\omega)$; and L_{np} are defined by:

$$L_{np}(t; \omega) = Y_n \left[\omega \int_0^t \frac{dt'}{1 + \omega^2 t'^2} \right] J_p \left[\omega \int_0^t \frac{dt'}{1 + \omega^2 t'^2} \right] - J_n \left[\omega \int_0^t \frac{dt'}{1 + \omega^2 t'^2} \right] Y_p \left[\omega \int_0^t \frac{dt'}{1 + \omega^2 t'^2} \right] : \quad (68)$$

The second equation of system (58) can then be used to obtain the other components of the velocity in the form:

$$\hat{v}_z(z) = \frac{h_1}{2} \int_0^z \frac{dt}{A} L_{00}(t; \omega) - \frac{h_2}{A} \int_0^z \frac{dt}{1 + \omega^2 t^2} L_{10}(t; \omega) ; \quad (69)$$

and a similar expression for $\hat{v}_y(z)$. We can now use equations (67) and (69) to calculate turbulence amplitude (x4.3.1) and transport (x4.3.2 and x4.3.3). Note that equations (67) and (69) are exact solutions valid for all values of ω .

4.3.1 Turbulence amplitude

From equations (67) and (69), we can easily obtain the turbulence amplitude as:

$$\begin{aligned} \overline{v_x^2} &= \frac{f}{4} \frac{\omega^2}{(2\omega)^3 A} \int_0^z d^3 k F(k) (1 + a^2) [X_1(k) + X_2(k)] ; \\ \overline{v_z^2} &= \frac{f}{4} \frac{\omega^2}{(2\omega)^3 A} \int_0^z d^3 k F(k) (1 + a^2) [X_3(k) + X_4(k)] : \end{aligned} \quad (70)$$

Here, for simplicity, we considered only an isotropic forcing, given by equation (24), and defined the following integrals:

$$\begin{aligned}
X_1(k) &= \int_a^{Z+1} \frac{e^{-2Q(\cdot)Q(a)}}{1+a^2} [L_{01}(a; \cdot)]^2 d\cdot; \\
X_2(k) &= \int_a^a \frac{e^{-2Q(\cdot)Q(a)}}{1+a^2} [L_{11}(a; \cdot)]^2 d\cdot; \\
X_3(k) &= \int_a^{Z+1} e^{-2Q(\cdot)Q(a)} [L_{00}(a; \cdot)]^2 d\cdot; \\
X_4(k) &= \int_a^{Z+1} e^{-2Q(\cdot)Q(a)} [L_{10}(a; \cdot)]^2 d\cdot;
\end{aligned} \tag{71}$$

Here, L_{np} 's are given by equation (68). We now consider the strong shear limit: $k_y^2 \rightarrow \infty$. As both Bessel functions become as $(1+a^2)^{-1/4}$ (up to a trigonometric functions) for large a , the first two integrals converge as $a \rightarrow \infty$. Thus, it is sufficient to put $a = 0$ in X_1 and X_2 in equation (71) to obtain the leading order behaviour for $a \rightarrow \infty$. In comparison, the integrand of X_3 and X_4 behaves as $1/a^2$ for $a \rightarrow \infty$, giving a contribution of order $\ln a$ to leading order.

We now examine the turbulence amplitude in the large rotation limit: $\Omega \rightarrow \infty$. To do so, we use the asymptotic behaviour of the integrals (71) derived in appendix B.1.2. Using equations (91) and (93) in equation (70), we obtain the following leading order contribution of the turbulent amplitude:

$$\begin{aligned}
\langle v_x^2 \rangle &= \frac{f}{(2\pi)^3 A} \int_a^Z d^3k F(k) \frac{P}{1+a^2}; \\
\langle v_z^2 \rangle &= \frac{f}{(2\pi)^3 A} \int_a^Z d^3k F(k) \frac{P}{1+a^2} \frac{\ln a}{3};
\end{aligned} \tag{72}$$

Thus, the turbulence amplitude is larger in the $y-z$ plane than the one in x direction by a logarithmic factor. Moreover, equation (72) shows that the turbulence amplitude does not depend on the rotation rate in the large rotation limit, being quenched only by shear. In particular, $\langle v_y^2 \rangle = \langle v_z^2 \rangle$. These results are the same as in the case where the shear and the rotation are perpendicular [see equation (26)] and thus agree with the WKB solution in the previous section.

4.3.2 Turbulent transport of momentum

We now calculate the turbulent viscosity τ defined by $\langle v_x v_y \rangle = -\tau \partial_x U_0 = -\tau A$. From equations (67) and (69), we can derive the Reynolds stress in the case of an isotropic forcing:

$$\langle v_x v_y \rangle = \frac{f}{4(2\pi)^3 A} \int_a^Z d^3k F(k) (1+a^2) [X_5(k) + X_6(k)]; \tag{73}$$

where,

$$\begin{aligned}
X_5(k) &= \int_a^{Z+1} \frac{e^{-2Q(\cdot)Q(a)}}{1+a^2} [L_{01}(a; \cdot)]^2 d\cdot; \\
X_6(k) &= \int_a^{Z+1} \frac{e^{-2Q(\cdot)Q(a)}}{1+a^2} [L_{11}(a; \cdot)]^2 d\cdot;
\end{aligned} \tag{74}$$

Here, L_{np} 's are again given by equation (68). Note that the expression for the transport of angular momentum [equation (73)] is the same as that of $h_{x_i}^2$ [equation (70)] except for the multiplicative factor of $\frac{1}{2}$. This is simply because, for $\Omega = 0$, the incompressibility condition imposes $\hat{v}_y = -\hat{v}_x$. By using the asymptotic behaviour of Bessel functions for large argument, we see that the two integrals X_5 and X_6 in equation (74) can be evaluated in the strong shear limit by just putting $\Omega = 0$. Consequently, the turbulent viscosity is of order A^{-2} for any value of Ω .

In the large rotation limit ($\Omega \gg 1$), we can estimate the integrals (74) and obtain the following turbulent viscosity:

$$\tau = \frac{f}{(2\Omega)^3 A^2} \int d^3k F(k) : \quad (75)$$

Equation (75) shows that the turbulent viscosity does not depend on rotation in the large rotation limit and is obviously negative. Note that this result is the same as in the perpendicular case [see equation (40)] and, thus again, agrees with the WKB solution found previously.

4.3.3 Particles transport

The fluctuating concentration of particles can be obtained by integration of the fluctuating velocities (67) and (69) [see equation (10)]. Then, the diagonal part of turbulent diffusivity can be obtained as:

$$D_T^{xx} = \frac{f}{4(2\Omega)^3 A^2} \int d^3k (1+a^2) F(k) [P_1(k) + P_2(k)] ; \quad (76)$$

$$D_T^{zz} = \frac{f}{4(2\Omega)^3 A^2} \int d^3k (1+a^2) F(k) [P_3(k) + P_4(k)] :$$

Here, we define integrals P_i which all have the following form :

$$P_i(k) = \int_a^{Z+1} d\bar{z} e^{2iQ(\bar{z})} F_i(\bar{z}) F_i(t) dt ; \quad (77)$$

for $i = 1$ to 4. The functions $F_i(\bar{z})$'s are defined by:

$$F_1 = \frac{L_{01}(a; \bar{z})}{\mathcal{P} \frac{1+a^2}{2}} ; \quad F_2 = \frac{L_{11}(a; \bar{z})}{\mathcal{P} \frac{1+a^2}{2}} ; \quad (78)$$

$$F_3 = L_{00}(a; \bar{z}) ; \quad F_4 = L_{10}(a; \bar{z}) :$$

In the large rotation limit ($\Omega \gg 1$), the F_i 's are oscillating functions. Thus, to evaluate integrals (77) in the strong shear limit ($\Omega \gg 1$), we can not simply put $\Omega = 0$ in equation (77) as is explained in the appendix B.3. A careful analysis (see appendix B.3) then gives us the following expression in the limits of strong shear ($\Omega \gg 1$) and large rotation ($\Omega \gg 1$):

$$D_T^{xx} = \frac{f}{8} \int_a^{Z+1} \frac{F(k)}{\mathcal{P} \frac{1+a^2}{2}} dk + \frac{f}{(2\Omega)^3 A} \int_{\bar{z} < 0} d^3k \frac{\mathcal{P}}{1+a^2 F(k)} ;$$

$$D_T^{zz} = \frac{f}{16} \int_a^{Z+1} \frac{F(k)}{\mathcal{P} \frac{1+a^2}{2}} dk + \frac{f}{(2\Omega)^3 A} \int_{a < 0} d^3k \frac{\mathcal{P}}{1+a^2 F(k)} : \quad (79)$$

		Perpendicular		Parallel	
		A	A	A	A
$h v_x^2 i$		1	$A^{-1} (1 + C)$	1	A^{-1}
$h v_y^2 i$	$h v_z^2 i$	$j \ln j$	$A^{-2=3} (1 + C) j \ln j$	$j \ln j$	$A^{-2=3}$
T		A^{-2}	A^{-2}	A^{-2}	A^{-2}
x		0	$A^{-2} j \ln j$	0	0
z		0	0	0	$A^{-4=3}$
D_T^{xx}		1	$A^{-2} (1 + C) j \ln j$	1	A^{-2}
D_T^{yy}	D_T^{zz}	1	$A^{-4=3} (1 + C) j \ln j$	1	$A^{-4=3}$

Table 1: Summary of our results obtained both for the perpendicular and parallel cases in the strong shear limit. In the perpendicular case, the rotation is in the z direction whereas it is in the x direction in the parallel case. In both cases, the shear is in the x direction. The C symbol stands for an additional constant of order 1.

The transport of particles in equation (79) involves two contributions, both of which scale as λ^{-1} for rapid rotation. The first contribution comes from the integration by parts and has to be kept only because T_0 can vanish for $a = 0$ while the second comes from the stationary point in the integration (see appendix B.3 for details). Note that the ratio of the second term to the first one is equal to $k^2 = A^{-2}$. Consequently, in the strong shear limit ($\lambda \rightarrow 1$), the first term dominates. Thus, the transport of particles is the same as the one found with the WKB analysis (see x4.1).

To summarise, in this section, we solved equation (58) exactly for $\lambda = 0$ and compared the results with the WKB analysis performed in x4.1 (which is valid only for $a > 0$). The results being the same, the conclusions reached from WKB analysis remain valid even if $a = 0$.

5 Discussion in the strong shear limit

In x3 and x4, depending on the values of the parameter $\lambda = A = (\frac{k}{\omega})$, we considered two regimes: the strong shear ($\lambda \rightarrow 1$) and the weak shear limits ($\lambda \rightarrow 0$). As the quasi-linear analysis is likely to be valid for sufficiently strong shear, we here summarise and discuss the results obtained in the limit of strong shear. Table 1 summarises our findings by highlighting the dependence of these quantities on the shearing rate A and the rotation rate (or their ratio, $\lambda = A^{-1}$). In the following, we discuss these results.

5.1 Stability of rotating shear flows

Our first result concerns the stability of shear flows in the presence of rotation. In the case where the rotation is perpendicular to the plane of the fluid motion (see figure 1), we recovered the Bradshaw criterion (Bradshaw, 1969). In our notation, it states that the configuration is unstable if $B = (1 - \Omega) < 0$ or, equivalently, if $\Omega = A$ lies in the interval $[0; 1]$. This result has already been reported by many authors, who showed not only that the maximum destabilisation occurs for $\Omega = 1/2$ but also that there is an important asymmetry with respect to $\Omega = 1/2$ which is not included in the Bradshaw criterion (Speziale & Mhisis, 1989; Cambon et al., 1994; Salhi & Cambon, 1997). This is because Bradshaw criterion can be recovered by a pressure-less analysis while the effect of pressure is to destroy this symmetry. We can easily show this asymmetry with respect to $\Omega = 1/2$ in our results: even if the equation (18) for the x-component of the velocity is symmetric with respect to $\Omega = 1/2$ (as it depends only on $b = \Omega^2 B$), equation (19) for the other components of the velocity are not because of the term proportional to $\Omega - 1/2$. In the parallel case (see figure 4), we found that the system was stable regardless of the values of shear and rotation.

5.2 Turbulence amplitude

The first two rows of Table 1 show that the turbulence amplitude in the direction of the shear (x) is more reduced by the shear than in the perpendicular one. This is true both for the large rotation limit, where they scale as Ω^{-1} and Ω^{-2} (recall that $\Omega = \frac{1}{2} A^{-1}$) respectively, and for the weak rotation limit, where they scale as A^{-1} and $A^{-2/3}$ respectively. These results thus imply an effectively stronger turbulence in the plane (y-z) than in the x-direction. This anisotropic reduction of turbulence amplitude is mainly due to the shear which increases the dissipation (anisotropically) by efficiently creating small-scale vortices in the x-direction. Furthermore, the turbulence amplitude is affected by the rotation only in the case where the rotation is perpendicular to the shear flow and in the weak rotation limit. This is because rotation affects the stability of shear flows only in this case, as mentioned previously. Here we recover the Bradshaw criterion: for $\Omega > 1/2$, a positive Ω tends to destabilise the turbulence (the kinetic energy is increased) whereas a negative value tends to stabilise the turbulence. For $\Omega < 1/2$, the effect of rotation on turbulence is weakly anisotropic, suppressing the turbulence in the y-z plane more than the one in the x-direction by a factor of $\ln 2$. As a result, the anisotropy due to shear flow is weakened by rotation. This reflects the tendency of rotation to lead to almost isotropic turbulence.

5.3 Transport of angular momentum

The transport of angular momentum was found to involve two contributions: the turbulent viscosity τ_T and the effect. The former is a diffusive transport making the effective viscosity to $\tau_T + \mu$ (μ is the molecular viscosity) while the latter is a non-diffusive momentum transport. Our results show that the turbulent viscosity does not depend on the relative orientation of the shear and rotation. We also found a transition from a negative viscosity, for large rotation,

to a positive viscosity, for weak rotation. This shows the influence of rotation to favour transfer of energy from small-scales to large-scales (inverse cascade). In comparison, the effect is a source of non-dissipative flux and prevents a uniform rotation to be solution of the averaged Reynolds equation. This term is present with an isotropic forcing in contrast with the case without shear where a source of anisotropy in the system is necessary for such an effect to appear. This is due to the fact that, even for an isotropic forcing, the shear induces anisotropy in the system as shown here and by Kim (2005). In the case of an anisotropic turbulence, it was shown that the effect was proportional to the anisotropy in the velocity field (Kichatinov, 1986; Rudiger, 1989). Here, in the perpendicular case, we found that the effect scales as $A^{-2} \ln j$ whereas the anisotropy in the velocity amplitude is given, at leading order, by A^{-4+3} . Consequently, the effect is smaller than the anisotropy in the turbulent velocity amplitude. This is because the anisotropy is not simply given here but has to be induced self-consistently by the shear during the evolution. Consequently, the anisotropy does not remain the same at all time and the resulting effect is smaller than the anisotropy in the velocity amplitude for large time. One can also note that the magnitude of the effect is not the same in the two cases. In the parallel case, it scales as A^{-4+3} while, in the perpendicular case, it scales as $A^{-2} \ln j$. Thus, the effect is larger in the parallel case than in the perpendicular case.

5.4 Transport of scalar

In the case of rapid rotation, we found that the transport of scalars is mainly governed by the rotation, scaling as ω^{-1} in all directions. The transport in the direction parallel to the rotation is twice larger than the one in the perpendicular direction (see equation (50) and Kichatinov et al., 1994) with a slight anisotropy. However, in the weak rotation limit, the transport of chemical species is reduced by shear with a stronger reduction in the direction parallel to the shear than in the perpendicular one (by a factor A^{-2} and A^{-4+3} respectively). Furthermore, there is a (weak) reduction due to rotation but only in the perpendicular case. These results are consistent with the calculations of Brethouwer (2005) as the anisotropy in the transport of particles is the same as that in the turbulent intensity. This is because, in the quasi-linear approximation, the rotation favours isotropy with the anisotropy of both quantities being caused by the shear only.

5.5 Effect of a bounded domain

In the calculation of all the turbulent coefficients in the weak shear limit (1) and also of the transport of particles in the strong shear limit (1), we obtained a result proportional to the following type of integral:

$$I(k; \omega) = \int \frac{H(k)}{2k^4 + \omega^2} d^3k; \quad (80)$$

where $\bar{\omega} = (\omega \cdot k) = \omega k \cos \theta$ is the projection of the unit vector in the direction of the wave number on the rotation axis. When the domain of integration is unbounded, the integration over the angular variable gives this integral proportional to ω^{-1} , when the rotation rate is sufficiently large [see equation (36-38) for details]. This is because this integral involves some contribution of order 1 (when $\theta = 0$) and others of magnitude ω^{-2} .

However, in most practical applications, the domain of integration in Fourier space is bounded. Thus there is a minimal wavenumber (corresponding to a maximum length, for instance the size of the box) in the direction of the rotation that we call $k_m = m \text{ in } (k_x)$. The preceding scaling in ω is valid when $\omega^2 k^6 \gg \nu^2 k_m^2$. In the opposite case, the term ω_0^2 in equation (80) is always dominant and we thus expect this integral to behave as ω^{-2} for large rotation rate.

5.6 Comparison with stratification

It is well known that compressibility can inhibit mixing and reduce energy amplification produced by a large-scale shear (see Simone et al., 1997, and references therein). Furthermore, the analogy between rotating and stratified flows (GreenSPAN, 1968), which has been used by Bradshaw (1969) to derive his criterion, can be used to comment on the case with shear and stratification. Salhi (2002) has shown that, by the normal analysis, the perpendicular case (studied here) is equivalent to the case with a stratification in the x-direction (except when $k_x = 0$). Thus, the stratified case in the x-direction is expected to be very similar to the case where the rotation is perpendicular to the plane of the flow. Indeed, in that case, we found (Kim & Leprovost, 2006) that the scaling of the turbulent intensity and the turbulent viscosity do not depend on the Brunt-Väisälä frequency N (which characterises the intensity of the stratification and thus plays the same role as ω in the rotating case) and have the same scalings as those given in the first column of Table 1. Kim & Leprovost (2006) also found that the transport of scalar was reduced proportional to N^{-2} , which corresponds to the case discussed in §5.5.

6 Conclusion

In this paper, we have performed a thorough investigation of the combined effects of shear and rotation on the structure of turbulence. While both rotation and (stable) shear flow tend to regulate turbulence, there are important differences in their effects, which should be emphasised. Rotation, by exciting inertial waves, tends to reduce turbulence transport more heavily than turbulence amplitude while shear flows reduce both of them to a similar degree. That is, rotation (or waves) quenches the cross-phase (normalised flux) more than shear flow does (Kim & Diamond, 2003; Kim, 2006). Furthermore, in sharp contrast with rotation, shear flow induces a strong anisotropic turbulence and transport (e.g. momentum transport, chemical mixing, etc.). On the other hand, rotation acting together with shear flow is shown to give rise to a novel, non-dissipative flux for momentum transport (the so-called effect) which transfers energy from the fluctuating velocity field to the large-scale flow. In comparison, the eddy viscosity from the dissipative part of momentum transport is found to be negative for strong shear and rotation.

These results can have significant implications for astrophysical and geophysical systems. In particular, the effect and/or negative viscosity can provide a mechanism for the generation of ubiquitous large-scale shear flows, which are often observed in these objects. Furthermore, the anisotropic mixing of scalars should be taken into account in understanding the surface depletion of light elements in stars (Pinsonneault, 1997).

Finally, we note that numerical confirmation of our prediction as well as the extension of our work to three-dimensional magnetohydrodynamics with rotation remain important problems, and will be addressed in future publications.

This work was supported by U.K. PPARC Grant No. PP/B501512/1.

A Decay of the homogeneous solution in the parallel case

In x4, we have seen that for sufficiently large τ , the solution of the first equation of equation (58) can be written:

$$\hat{v}_x(\tau) = \frac{1}{\tau^{\frac{h}{2}}} \left[A J_1(j\tau^{\frac{h}{2}}) + B Y_1(j\tau^{\frac{h}{2}}) \right] \quad (81)$$

Here, the two constants can be calculated at a given time τ_c that is large enough ($\tau_c = \tau$) in the form:

$$\begin{aligned} A &= C Y_2(j\tau_c^{\frac{h}{2}}) - D Y_1(j\tau_c^{\frac{h}{2}}) \\ B &= C J_2(j\tau_c^{\frac{h}{2}}) + D J_1(j\tau_c^{\frac{h}{2}}); \end{aligned} \quad (82)$$

where we defined the new coefficients:

$$\begin{aligned} C &= \frac{j\tau_c^{\frac{h}{2}}}{2} \hat{v}_x(\tau_c); \\ D &= \frac{(\tau_c^{\frac{h}{2}})^{3-2}}{2\tau_c} \hat{v}_x^0(\tau_c) = \frac{\tau_c^{\frac{h}{2}}}{2} (\hat{v}_y(\tau_c) - \hat{v}_z(\tau_c)) - 2\hat{v}_z(\tau_c); \end{aligned} \quad (83)$$

Then, we can use the second equation of (58) to obtain the velocity in the z-direction for large time (for $\tau = \tau_c$) as:

$$\begin{aligned} \hat{v}_z(\tau) &= \hat{v}_z(\tau_c) + \int_{\tau_c}^{\tau} \left[-\hat{v}_z(\tau) - c\hat{v}_x(\tau) \right] dt \\ &= \hat{v}_z(\tau_c) - \hat{v}_z(\tau_c) - c\hat{v}_x(\tau_c) - \int_{\tau_c}^{\tau} \left[A J_0(j\tau^{\frac{h}{2}}) + B Y_0(j\tau^{\frac{h}{2}}) \right] dt; \end{aligned} \quad (84)$$

Here, ϵ is the sign of τ . Equation (84) shows that the velocity in the z-direction tends to approach a finite limit $\hat{v}_z(\tau \rightarrow \infty)$ as $\tau \rightarrow \infty$. To calculate this limit, we need to calculate the term in large square brackets in equation (84) for $\tau = \tau_c$. In the following, we call this term E. Plugging equation (82) in the E, we obtain the following:

$$E = \frac{2C}{j\tau_c^{\frac{h}{2}} + \tau_c^{\frac{h}{2}}} + D \frac{2}{j\tau_c^{\frac{h}{2}} + \tau_c^{\frac{h}{2}}}; \quad (85)$$

Finally, using this result, we can obtain $\hat{v}_z(\tau \rightarrow \infty)$ as follows:

$$\begin{aligned} \hat{v}_z(\tau \rightarrow \infty) &= \hat{v}_z(\tau_c) + \int_{\tau_c}^{\infty} \left[-\hat{v}_z(\tau) - c\hat{v}_x(\tau) \right] dt \\ &= -[c\hat{v}_x(\tau_c) + \hat{v}_y(\tau_c) + \hat{v}_z(\tau_c)] = 0; \end{aligned} \quad (86)$$

because of incompressibility. Then, by incompressibility, $\hat{v}_y \rightarrow 0$ when $\tau \rightarrow \infty$.

B A sym ptotic expansion of integrals

In x4.3, we took a large shear limit ($\epsilon \rightarrow 1$) and obtain equation (70) for the turbulence intensity, equation (73) for the transport of angular momentum, and equation (76) for the transport of particles in terms of integrals involving Bessel functions of an argument depending on the rotation. We here derive asymptotic behaviour of these integrals to simplify our results.

B.1 Non oscillating integrands

For non oscillating integrands, it is sufficient to put $\epsilon = 0$ in the integrals to find the large shear limit (the resulting integral converges as $\epsilon \rightarrow 0$). Here, we provide asymptotic behaviour of the following integrals for small or large ϵ_0 :

$$\begin{aligned} X_1(k) &= \int_0^{Z+1} \frac{1}{1+\epsilon^2} [L_{0,1}(t; \epsilon)]^2 dt; & (87) \\ X_2(k) &= \int_0^{Z+1} \frac{1}{1+\epsilon^2} [L_{11}(a; \epsilon)]^2 dt; \\ X_5(k) &= \int_0^{Z+1} \frac{1}{1+\epsilon^2} [L_{01}(t; \epsilon)]^2 dt; \\ X_6(k) &= \int_0^a \frac{1}{1+\epsilon^2} [L_{11}(a; \epsilon)]^2 dt; \end{aligned}$$

Here L_{np} 's are given by equation (68)

B.1.1 Small rotation limit ($\epsilon_0 \rightarrow 1$)

To calculate X_1 and X_5 , one can use the asymptotic expansion of the Bessel functions and readily obtain:

$$\begin{aligned} X_5 &= \frac{4}{2^{\frac{1}{2}} \epsilon_0^{\frac{1}{2}}} \int_0^{Z+1} \frac{d}{(1+\epsilon^2)^2} = \frac{2}{2^{\frac{1}{2}} \epsilon_0^{\frac{1}{2}}} \frac{h}{2} \arctan(a) \frac{a}{1+a^2}; & (88) \\ X_5 &= \frac{4}{2^{\frac{1}{2}} \epsilon_0^{\frac{1}{2}} a} \int_0^{Z+1} \frac{d}{(1+\epsilon^2)^2} = \frac{2}{2^{\frac{1}{2}} \epsilon_0^{\frac{1}{2}} (1+a^2)}; \end{aligned}$$

If we apply the same strategy to the calculations of X_2 and X_6 , the resulting expression would not be integrable so we have to calculate it otherwise:

$$\begin{aligned} X_3 &= \frac{2}{\epsilon_0^{\frac{1}{2}} (1+a^2)^{\frac{1}{2}}} \int_0^{Z+1} \frac{J_1^2(\epsilon_0 \sqrt{1+\epsilon^2})}{1+\epsilon^2} dt = \frac{2}{\epsilon_0^{\frac{1}{2}} (1+a^2)^{\frac{1}{2}}} \int_0^a \frac{J_1^2(\sqrt{\frac{\epsilon_0^2}{2} + x^2})}{\frac{\epsilon_0^2}{2} + x^2} dx & (89) \\ &= \frac{2}{\epsilon_0^{\frac{1}{2}} (1+a^2)^{\frac{1}{2}}} \int_0^{Z+1} \frac{J_1^2(x)}{x^2} \frac{1}{3^{\frac{1}{2}} \epsilon_0^{\frac{1}{2}} (1+a^2)^{\frac{1}{2}}}; \\ X_6 &= \frac{2}{\epsilon_0^{\frac{1}{2}} (1+a^2)^{\frac{1}{2}}} \int_0^a \frac{J_1^2(\epsilon_0 \sqrt{1+\epsilon^2})}{1+\epsilon^2} dt = \frac{2}{\epsilon_0^{\frac{1}{2}} (1+a^2)^{\frac{1}{2}}} \int_0^{Z+1} \frac{J_1^2(x)}{x} \frac{1}{\epsilon_0^{\frac{1}{2}} (1+a^2)^{\frac{1}{2}}}; \end{aligned}$$

B.1.2 Large rotation limit ($\theta \rightarrow 1$)

Using the Bessel asymptotic behaviour for large argument, we obtain the following formula for the first integral:

$$X_1 = \frac{4}{2} \int_0^{Z+1} \frac{\cos^2 \left(\sqrt{1+a^2} \sqrt{1+\frac{y}{2}} \right)}{(1+\frac{y}{2})^{3/2}} dy \quad (90)$$

$$\frac{2}{2} \int_0^{Z+1} \frac{1}{(1+\frac{y}{2})^{3/2}} dy = \frac{2}{2} \int_0^{Z+1} \frac{1}{1+\frac{y}{2}} dy ;$$

and similarly for the other three integrals. Finally, we obtain the following asymptotic behaviour for the four integrals (87):

$$X_1 = X_2 = \frac{2}{2} \int_0^{Z+1} \frac{1}{1+\frac{y}{2}} dy = \ln \left(1 + \frac{Z+1}{2} \right) ; \quad (91)$$

$$X_5 = X_6 = \frac{2}{2} \int_0^{Z+1} \frac{1}{1+\frac{y}{2}} dy ;$$

B.2 Logarithmic divergence

As noticed in 4.3.1, there is a logarithmic divergence arising in the calculation of X_3 and X_4 . We here calculate this divergence in the case of a fast oscillation. Following Kim (2005), we change the integration variable from θ to $y = 2\theta^3 = 3$, replace the Bessel function by the expression valid for large argument ($\theta \rightarrow 1$), and then obtain the following, to leading order in θ :

$$X_3(k_1) = \frac{2}{a^3} \int_0^{Z+1} \frac{e^{-y} dy}{(3y)^{2/3} (2)^{1/3} \left(1 + \frac{3y}{2} \right)^{2/3}} \quad (92)$$

$$\approx \frac{2}{a^3} \int_0^{Z+1} \frac{e^{-y} dy}{(3y)^{2/3} (2)^{1/3} \left(1 + \frac{3y}{2} \right)^{2/3}} = \frac{2}{a^3} \int_0^{Z+1} \frac{e^{-y} dy}{(3y)^{2/3} (2)^{1/3} \left(1 + \frac{3y}{2} \right)^{2/3}} = \frac{2}{a^3} \int_0^{Z+1} \frac{e^{-y} dy}{(3y)^{2/3} (2)^{1/3} \left(1 + \frac{3y}{2} \right)^{2/3}} = \frac{2}{a^3} \int_0^{Z+1} \frac{e^{-y} dy}{(3y)^{2/3} (2)^{1/3} \left(1 + \frac{3y}{2} \right)^{2/3}} ;$$

We see that as θ tends to zero, the integrand in equation (92) becomes proportional to $1/y$, giving a contribution of the order \ln .

In the large rotation limit ($\theta \rightarrow 1$), we replace the Bessel functions by their asymptotic behaviour to obtain:

$$X_3 = \frac{4}{2} \int_0^{Z+1} \frac{e^{-y} dy}{(3y)^{2/3} (2)^{1/3} \left(1 + \frac{3y}{2} \right)^{2/3}} \frac{\sin^2 \left(\sqrt{1+a^2} \sqrt{1+\frac{y}{2}} \right)}{1 + \frac{y}{2}} \quad (93)$$

$$\frac{2}{2} \int_0^{Z+1} \frac{1}{(3y)^{2/3} (2)^{1/3} \left(1 + \frac{3y}{2} \right)^{2/3}} \frac{e^{-y} dy}{1 + \frac{y}{2}} = \frac{2}{2} \int_0^{Z+1} \frac{1}{(3y)^{2/3} (2)^{1/3} \left(1 + \frac{3y}{2} \right)^{2/3}} \frac{e^{-y} dy}{1 + \frac{y}{2}} ;$$

to leading order in θ . Following the same analysis, we find the same asymptotic behaviour for X_4 .

B.3 Oscillating integrands

The calculation of the transport of particles involves the computation of double integrals of the type:

$$P = \int_a^{Z+1} \int_a^Z e^{2iQ(\theta) - Q(a)} F(\theta) F(t) dt ; \quad (94)$$

where the functions F contains an oscillating functions. We here derive the asymptotic behaviour of this integral with $F(t) = f(t) \cos[\omega_0(t)]$ and the phase given by $\phi(t) = \int_0^t \frac{v}{1+a^2} dt$. The difficulty associated with the calculation of such integral is the presence of a point of stationary phase $t = 0$ where the integral cannot be done with an integration by part.

For $a > 0$, the point of stationary phase is never reached and then, the first integral can be approximated, for $\omega_0 \gg 1$, as:

$$I(\omega_0) \approx \int_a^Z \frac{F(t) dt}{1+a^2} \sin[\omega_0 \phi(t)] : \quad (95)$$

Using this approximation, P can be computed with the following result:

$$P \approx \frac{f(a)^2 (1+a^2)}{4[(1+a^2)^2 + \omega_0^2 a^2]} : \quad (96)$$

Note that the result is the same as in the perpendicular case where the integral defining the transport of particles does not involve any stationary point.

For $a < 0$, the behaviour of the integral $I(\omega_0)$ is affected by the stationary point in the vicinity of $\phi = 0$. We can however find an approximation as:

$$I(\omega_0) \approx \begin{cases} \int_0^{\infty} \frac{F(t) dt}{1+a^2} \sin[\omega_0 \phi(t)] & \text{if } \omega_0 \gg \frac{1}{|a|} ; \\ I_0 + c \int_0^{\infty} \frac{F(t) dt}{1+a^2} \sin[\omega_0 \phi(t)] & \text{if } j < \frac{1}{|a|} ; \\ 2I_0 \int_0^{\infty} \frac{F(t) dt}{1+a^2} \sin[\omega_0 \phi(t)] & \text{if } \omega_0 \ll \frac{1}{|a|} : \end{cases} \quad (97)$$

Here, $I_0 = \int_0^{\infty} F(t) dt$ is the value given by the stationary point and $c = f(0) \cos[\omega_0 \phi(0)]$ is obtained by Taylor expanding I in the vicinity of $\phi = 0$. Figure 5 shows the numerical computation of the integral compared to the approximation (97) and shows an excellent agreement. Using equation (97), we obtain P as:

$$P \approx \frac{f(a)^2 (1+a^2)}{4[(1+a^2)^2 + \omega_0^2 a^2]} + 2I_0^2 : \quad (98)$$

The first contribution comes from the integration by part (and as the result is odd in ϕ , the contributions from $\phi = 0$ and $\phi = \pi$ cancel out). The second contribution (of order ω_0^{-1}) comes from the stationary point. Both contributions have to be kept as the first one can be important if $|a| \ll 1$.

For $a = 0$, the stationary point counts twice as less, so the approximation becomes:

$$I(\omega_0) \approx \begin{cases} c \int_0^{\infty} \frac{F(t) dt}{1+a^2} \sin[\omega_0 \phi(t)] & \text{if } 0 < \omega_0 \ll \frac{1}{|a|} \\ I_0 \int_0^{\infty} \frac{F(t) dt}{1+a^2} \sin[\omega_0 \phi(t)] & \text{if } \omega_0 \gg \frac{1}{|a|} \end{cases} \quad (99)$$

In that case, the contribution from the stationary point cancels out as $I(0) = 0$. Therefore, for $a = 0$, the only contribution comes from the end point of the integration and is the same as for $a > 0$ [see equation (96)].

Performing the same procedure when $F(t) = f(t) \sin[\omega_0(t)]$, we obtain the following result:

$$P \approx \frac{f(a)^2 (1+a^2)}{4[(1+a^2)^2 + \omega_0^2 a^2]} + \frac{f(a)^2 (1+a^2)}{4[(1+a^2)^2 + \omega_0^2 a^2]} \quad (100)$$

$$+ \frac{1}{\omega_0} f(0)^2 \sin^2[\omega_0 \phi(0)] ; \quad (101)$$

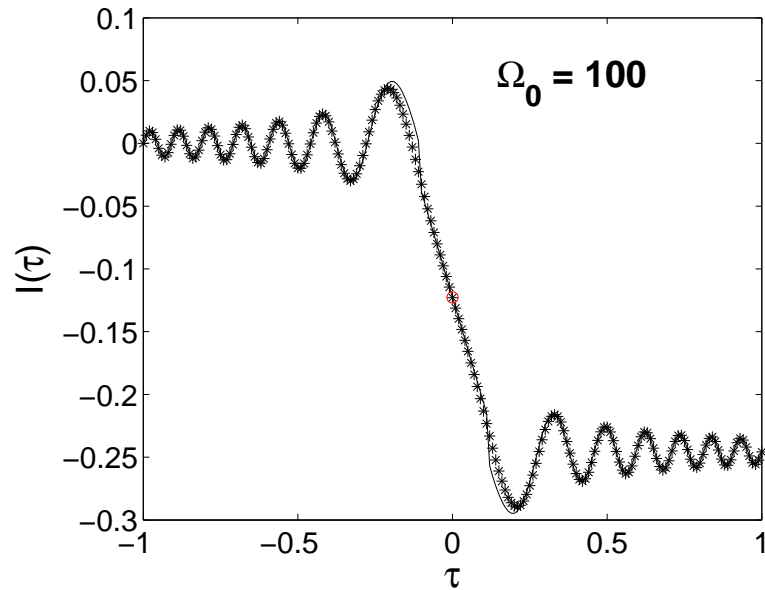


Figure 5: Graph of the function $I(\tau)$ with our approximation θ_7 . The parameters are $a = 1$ and $\Omega_0 = 100$.

the second line being present only if $a < 0$ (i.e. when the point of stationary phase is reached).

References

- Bech, K. H. & Andersson, H. I. 1996 Secondary flow in weakly rotating turbulent plane Couette flow. *J. Fluid Mech.* 317, 195{214.
- Bech, K. H. & Andersson, H. I. 1997 Turbulent Couette plane flow subject to strong system rotation. *J. Fluid Mech.* 347, 289{314.
- Bender, C. M. & Orszag, S. A. 1975 *Advanced mathematical methods for scientists and engineers*. McGraw Hill.
- Bradshaw, P. 1969 The analogy between stream line curvature and buoyancy in turbulent shear flow. *J. Fluid Mech.* 36, 177{191.
- Brethouwer, G. 2005 The effect of rotation on rapidly sheared homogeneous turbulence and passive scalar transport. Linear theory and direct numerical simulation. *J. Fluid Mech.* 542, 305{342.
- Cambon, C., Benoit, J. P., Shao, L. & Jacquín, L. 1994 Stability analysis and large-eddy simulation of rotating turbulence with organized eddies. *J. Fluid Mech.* 278, 175{200.
- Cambon, C., Mansour, N. N. & Godeferd, F. S. 1997 Energy transfer in rotating turbulence. *J. Fluid Mech.* 337, 303{332.

- Frisch, U., She, Z. S. & Sulem, P. L. 1987 Large-scale flow driven by the anisotropic kinetic alpha effect. *Physica D* 28, 382{392.
- Goldreich, P. & Lynden-Bell, D. 1964 II. Spiral arms as sheared gravitational instabilities. *MNRAS* 130, 125{158.
- Gradshteyn, I. S. & Ryzhik, I. M. 1965 Table of integrals series and products. Academic press.
- Greenspan, H. P. 1968 The theory of rotating fluids. CUP.
- Johnston, J. P., Halleen, R. M. & Lezius, D. K. 1972 Effects of spanwise rotation on structure of 2 dimensional fully developed turbulent channel flow. *J. Fluid Mech.* 56, 533{557.
- Kichatinov, L. L. 1986 Turbulent transport of angular momentum and differential rotation. *Geophys. Astrophys. Fluid Dyn.* 35, 93{110.
- Kichatinov, L. L. 1987 A mechanism of differential rotation based on angular momentum transport by compressible convection. *Geophys. Astrophys. Fluid Dyn.* 38, 273{292.
- Kichatinov, L. L., Pipin, V. V. & Rudiger, G. 1994 Turbulent viscosity, magnetic diffusivity, and heat conductivity under the influence of rotation and magnetic field. *Astron. Nachr.* 315, 157{170.
- Kim, E. 2005 Self-consistent theory of turbulent transport in the solar tachocline. I. Anisotropic turbulence. *Astron. Astrophys.* 441, 763{772.
- Kim, E. 2006 Consistent theory of turbulent transport in two-dimensional magnetohydrodynamics. *Phys. Rev. Lett.* 96, 084504.
- Kim, E. & Diamond, P. H. 2003 Effect of mean flow shear on cross phase and transport reconsidered. *Phys. Rev. Lett.* 91 (7), 075001.
- Kim, E. & Dubrulle, B. 2001 Turbulent transport and equilibrium profiles in two-dimensional magnetohydrodynamics with background shear. *Phys. Plasmas* 8 (3), 813{824.
- Kim, E. & Leprovost, N. 2006 Self-consistent theory of turbulent transport in the solar tachocline. III. stratification. Submitted to *Astron. Astrophys.*
- Kippenhahn, R. 1963 Differential rotation in stars with convective envelopes. *Astrophys. J.* 137, 664{678.
- Kristoffersen, R. & Andersson, H. I. 1993 Direct simulations of low-Reynolds-number turbulent flow in a rotating channel. *J. Fluid Mech.* 256, 163{197.
- Lebedinsky, A. I. 1941 Rotation of the sun. *Astron. Zh.* 18, 10.
- Leblanc, S. & Cambon, C. 1997 On the three-dimensional instabilities of plane flows subjected to Coriolis force. *Phys. Fluids* 9 (5), 1307{1316.
- Lee, J. M., Kim, J. & Moin, P. 1990 Structure of turbulence at high shear rate. *J. Fluid Mech.* 216, 561{583.

- Leprovost, N. & Kim, E. 2006 Self-consistent theory of turbulent transport in the solar tachocline. II. tachocline convection. *Astron. Astrophys.* 456 (2), 617{621.
- Leprovost, N. & Kim, E. 2007 Effect of Rossby and Alfvén waves on the dynamics of the tachocline. *Astrophys. J.* 654, 1166.
- Métais, O., Flores, C., Yanase, S., Riley, J. J. & Lesieur, M. 1995 Rotating free-shear flows. 2. Numerical simulations. *J. Fluid Mech.* 293, 47{80.
- Moﬀatt, H. K. 1978 Magnetic field generation in fluids. CUP.
- Parker, E. N. 1955 Hydromagnetic dynamo models. *Astrophys. J.* 122, 293{314.
- Pedley, T. J. 1969 On instability of viscous flow in a rapidly rotating pipe. *J. Fluid Mech.* 35, 97{115.
- Pedlovsky, J. 1987 Geophysical fluid dynamics. Springer-Verlag.
- Pinsonneault, M. 1997 Mixing in stars. *Annu. Rev. Astron. Astrophys.* 35, 557{605.
- Proudman, J. 1916 On the motion of solids in a liquid possessing vorticity. *Proc. R. Soc. Lond. A* 92, 408{424.
- Rogers, M. M., Mansour, N. N. & Reynolds, W. C. 1989 An algebraic model for the turbulent flux of a passive scalar. *J. Fluid Mech.* 203, 77{101.
- Rüdiger, G. 1980 Reynolds stresses and differential rotation I. On recent calculations of zonal fluxes in rotating stars. *Geophys. Astrophys. Fluid Dyn.* 16, 239{261.
- Rüdiger, G. 1989 Differential rotation and stellar convection. Gordon and Breach.
- Salhi, A. 2002 Similarities between rotation and stratification effects on homogeneous shear flow. *Theoret. Comput. Fluid Dyn.* 7, 339{358.
- Salhi, A. & Cambon, C. 1997 An analysis of rotating shear flow using linear theory and DNS and LES results. *J. Fluid Mech.* 347, 171{195.
- Simone, A., Coleman, G. N. & Cambon, C. 1997 The effect of compressibility on turbulent shear flow: a rapid-distortion-theory and direct-numerical-simulation study. *J. Fluid Mech.* 330, 307{338.
- Sipp, D. & Jacquin, L. 2000 Three-dimensional centrifugal-type instabilities of two-dimensional flows in rotating systems. *Phys. Fluids* 12 (7), 1740{1748.
- Smith, L. M. & Waleffe, F. 1999 Transfer of energy to two-dimensional large scales in forced, rotating three-dimensional turbulence. *Phys. Fluids* 11 (6), 1608{1622.
- Speziale, C. G. & Mhisis, N. Mac Givolla 1989 Scaling laws for homogeneous turbulent shear flow in a rotating frame. *Phys. Fluids A* 1, 294{301.

- Steenbeck, M. & Krause, F. 1966 The generation of stellar and planetary magnetic fields by turbulent dynamo action. *Z. Naturforsch., Teil A* 21, 1285-1296, English translation: Roberts and Styx (1971) pp. 147-220.
- Tavoularis, S. & Corrsin, S. 1981 Experiments in nearly homogeneous turbulent shear flow with a uniform mean temperature gradient. Part 1. *J. Fluid Mech.* 104, 311-347.
- Taylor, G. I. 1921 Experiments on the motion of solids bodies in rotating fluids. *Proc. R. Soc. Lond. A* 104, 213-218.
- Townsend, A. A. 1976 *The structure of turbulent shear flow*, 2nd edn. CUP.
- Tritton, D. J. 1992 Stabilization and destabilization of turbulent shear-flow in a rotating fluid. *J. Fluid Mech.* 241, 503-523.
- Yanase, S., Flores, C., Metais, O. & Riley, J. J. 1993 Rotating free-shear flows. 1. Linear stability analysis. *Phys. Fluids A* 5 (11), 2725-2737.